Evaluation of Kilfrost GEO Antifreeze Performance in Ground Source Heat Pump Closed Loop Fields

NEW YORK STATE OF OPPORTUNITY. | NYSERDA

NYSERDA's Promise to New Yorkers:

NYSERDA provides resources, expertise, and objective information so New Yorkers can make confident, informed energy decisions.

Our Vision:

New York is a global climate leader building a healthier future with thriving communities; homes and businesses powered by clean energy; and economic opportunities accessible to all New Yorkers.

Our Mission:

Advance clean energy innovation and investments to combat climate change, improving the health, resiliency, and prosperity of New Yorkers and delivering benefits equitably to all.

Evaluation of Kilfrost GEO Antifreeze Performance in Ground Source Heat Pump Closed Loop Fields

Final Report

Prepared for:

New York State Energy Research and Development Authority

Albany, NY

Robert Carver
Senior Project Manager

Prepared by:

Kilfrost Limited

Haltwhistle, UK

Jerry Lewis
Chief Technical Officer

In partnership with:

Aztech Geothermal

Ballston Spa, NY

John Ciovacco
President

and

Ground Energy Support LLC

Durham, NH

J. Matt Davis
Chief Technical Officer

Notice

This report was prepared by Kilfrost Limited in partnership with Aztech Geothermal and Ground Energy Support LLC in the course of performing work contracted for and sponsored by the New York State Energy Research and Development Authority (hereafter "NYSERDA"). The opinions expressed in this report do not necessarily reflect those of NYSERDA or the State of New York, and reference to any specific product, service, process, or method does not constitute an implied or expressed recommendation or endorsement of it. Further, NYSERDA, the State of New York, and the contractor make no warranties or representations, expressed or implied, as to the fitness for particular purpose or merchantability of any product, apparatus, or service, or the usefulness, completeness, or accuracy of any processes, methods, or other information contained, described, disclosed, or referred to in this report. NYSERDA, the State of New York, and the contractor make no representation that the use of any product, apparatus, process, method, or other information will not infringe privately owned rights and will assume no liability for any loss, injury, or damage resulting from, or occurring in connection with, the use of information contained, described, disclosed, or referred to in this report.

NYSERDA makes every effort to provide accurate information about copyright owners and related matters in the reports we publish. Contractors are responsible for determining and satisfying copyright or other use restrictions regarding the content of reports that they write, in compliance with NYSERDA's policies and federal law. If you are the copyright owner and believe a NYSERDA report has not properly attributed your work to you or has used it without permission, please email print@nyserda.ny.gov

Information contained in this document, such as web page addresses, are current at the time of publication.

Abstract

This study was undertaken to evaluate the performance of a novel antifreeze (Kilfrost GEO) and its potential to improve the performance of ground source heat pump (GSHP) systems while reducing installation and operating costs for residents of New York State. An experimental apparatus was designed and built at the Hudson Valley Community College TEC-SMART facility to compare the performance of Kilfrost GEO against a commonly used antifreeze, propylene glycol, using the same set of experimental conditions. While the experimental study was limited by available time and a single design intent, sufficient data has been obtained to allow the construction of a model to support the comparison studies necessary to achieve the objectives of this work program.

Based on the test results, it is projected that Kilfrost Geo will reduce pumping energy by 6% annually while providing freeze protection at 15 degrees F compared to propylene glycol with freeze protection of only 20 degrees F. Kilfrost Geo also provides improved heat transfer characteristics at cold temperature that could reduce borehole lengths. Based on computer simulations, Kilfrost Geo's improved heat transfer characteristics has the potential to reduce borehole lengths by as much as 27%. This low temperature performance also mitigates common risks associated with GSHP deployment, allowing more confidence in this technology.

Keywords

Acknowledgements

Table of Contents

List of Figures

List of Tables

Acronyms and Abbreviations

COP	Coefficient of Performance
Dn	Dean number
DR	Diameter ratio of pipe
EWT	Entering water temperature
FM	Flow meter
FP	Freeze protection
gpm	Gallons per minute
GSHP	Ground source heat pump
HDPE	High density polyethylene
kWh	Kilowatt hour
LWT	Leaving water temperature
Nu	Nusselt number
PG	Propylene glycol
PP	Pumping power
Pr	Prandtl number
PT	Pressure transducer
psi	Pounds per square inch
Re	Reynolds number
SAGGL	Simulated above-ground ground loop
TW	Thermal well (with temperature sensor)
TS	Temperature sensor (on pipe)
W	Watts

Equation Symbols

d_i	inside diameter of pipe
f	friction coefficient
L	pipe length
g	gravitational acceleration constant
ϵ	pipe roughness coefficient
λ	dimensionless curvature
ρ	fluid density
μ	dynamic viscosity
v	average velocity

Executive Summary

This study was undertaken to evaluate the performance of a novel antifreeze (Kilfrost GEO) and its potential to improve the performance of ground source heat pump (GSHP) systems while reducing installation and operating costs for residents of New York State. An experimental apparatus was designed and built at the Hudson Valley Community College TEC-SMART facility to compare the performance of Kilfrost GEO against a commonly used antifreeze, propylene glycol, using the same set of experimental conditions.

While the experimental study was limited by available time and a single design intent, sufficient data has been obtained to allow the construction of a model to support the comparison studies necessary to achieve the objectives of this work program. Careful consideration of widely available and industry relevant standards and literature has helped to confirm the robustness of the findings reported here. These include the International Ground Source Heat Pump Association (IGSHPA) design manual as well as publications in the professional and scientific literature.

When comparing Kilfrost GEO to the more traditional antifreeze/heat transfer fluids that use propylene glycol, the benefits and utility of Kilfrost GEO can be realized through:

- The provision of freeze protection at 15°F and energy savings of 6% compared to propylene glycol with a freeze protection of 20°F. When comparing Kilfrost GEO with propylene glycol at the same 20°F freeze point, electricity savings would range from 11 to 15%.
- Improved heat transfer characteristics that could reduce borehole lengths.
- A reliability in operation that mitigates common risks associated with GSHP deployment, allowing more confidence in this technology.

Results of computer simulations suggest that Kilfrost Geo's improved heat transfer characteristics have the potential to reduce borehole lengths by as much as 27%. These results should be validated with actual field testing prior to being adopted as a new design practice.

In summary, Kilfrost GEO has a viscosity profile and heat carrying capacity that is better than propylene glycol, presenting opportunities for lower energy costs and other GSHP system design benefits. In performance terms, Kilfrost GEO performance approaches that of aqueous methanol, but without the risks of flammability or toxicity of the latter.

1   Introduction

New York State is seeking to make renewable energy technologies more affordable and accessible to its residents. One technology that offers the potential to deliver these goals is ground source heat pump (GSHP) technology, sometimes referred to as geothermal heat pumps (GHP) or simply geothermal. The most common applications of GSHP systems consist of circulating a heat transfer fluid through a series of pipes in the ground, and then converting this low-grade heat into usable energy with a heat pump. While the engineering technology of these systems has improved considerably over recent years, there remain relatively few options for the heat transfer fluid in these systems. The fluids that are currently available in the market are based on either propylene glycol which is nontoxic but relatively viscous (consuming more pumping energy), or methanol based, which offers a lower viscosity at reduced temperatures but has a high mammalian toxicity (considered to be a groundwater toxin) and is flammable under certain circumstances.

Kilfrost GEO is a novel heat transfer fluid that is based on food safe ingredients including sustainable and renewable materials. In addition, it has a low viscosity profile in use. This combination makes Kilfrost GEO a nontoxic and energy efficient option for reducing energy consumption while also providing for efficient heat transfer in cold conditions.

1.1   Objectives

This project evaluates technical data collected in Northeastern United States to compare Kilfrost GEO with the primary alternative fluids (i.e., propylene glycol-based fluids) used in many water-based, load side HVAC distribution systems and also on the source side of GSHP systems. The study focuses on comparing propylene glycol and Kilfrost GEO solutions as heat transfer fluids under conditions typical of a ground heat exchanger (GHX) and acting as the source side of GSHP systems—taking into consideration how those differences may affect GSHP system design and operation.

First, we undertake highly controlled lab-scale experiments using GSHP system equipment and operating conditions commonly observed for seasonal flow loop temperatures. The lab experiments focus on maintaining the same test conditions while only changing the antifreeze solution. These data are then used to validate models of pressure losses for the different antifreeze solutions over a range of operating temperatures. The models then allow for an evaluation of how Kilfrost GEO may impact GSHP system design and improve reliability under adverse operating conditions.

1.2   Previous Studies

In the design of a GSHP ground loop heat exchanger, the designer must balance several factors to optimize system performance. For systems with closed-loop heat exchangers (horizontal, vertical, or pond), antifreeze in the heat transfer fluid extends the range of heat exchanger operating temperatures so that the system can operate below 32°F. While it is often desirable to design systems so that they rarely drop below 32°F, the bi-national standard for GSHP system design (ANSI/CSA, 2016) allows for lower loop temperatures in many parts of NYS. The choice of antifreeze as it relates to the performance of a GSHP system is also well recognized in design manuals (IGSPHA Residential and Light Commercial Design) and industry literature (e.g., Gehlin and Spitler, 2015; Gagne-Boisvert and Bernier, 2017).

For example, when determining a flow rate and pipe size for a ground heat exchanger, common design practices call for maintaining turbulent flow in the pipe, to enhance thermal exchange with the ground, while limiting the flow rate so that the head loss is no greater than 4 feet of head per 100 feet of pipe (IGSHPA, 2011). While the additional head loss due to higher viscosity can be reduced by decreasing the flow rate, the flow in the ground loop should remain high enough to maintain turbulence. This operational range for ground loop flow is illustrated in the IGSHPA Residential and Light Commercial Design Manual (Figure 1). As shown in Figure 1, for a given pipe size, the range of flow rate decreases for higher viscosity antifreeze solutions (e.g., propylene glycol) compared to methanol at similar levels of freeze protection. For small pipe sizes, that are very common in horizontal loops, when the fluid temperature is 25°F, the lower-viscosity methanol solution allows for a larger range of flows (approximately 2 gallons per minute (gpm)), in which flow remains turbulent but without exceeding a head loss of 4 feet per 100 feet of pipe. For the same small pipe size (3/4 inch), the operating range for the propylene glycol solution is reduced to approximately 0.5 gpm.

Figure 1. Flow Rate Ranges for Different Heat Exchange Fluids [from IGSPHA, 2011]
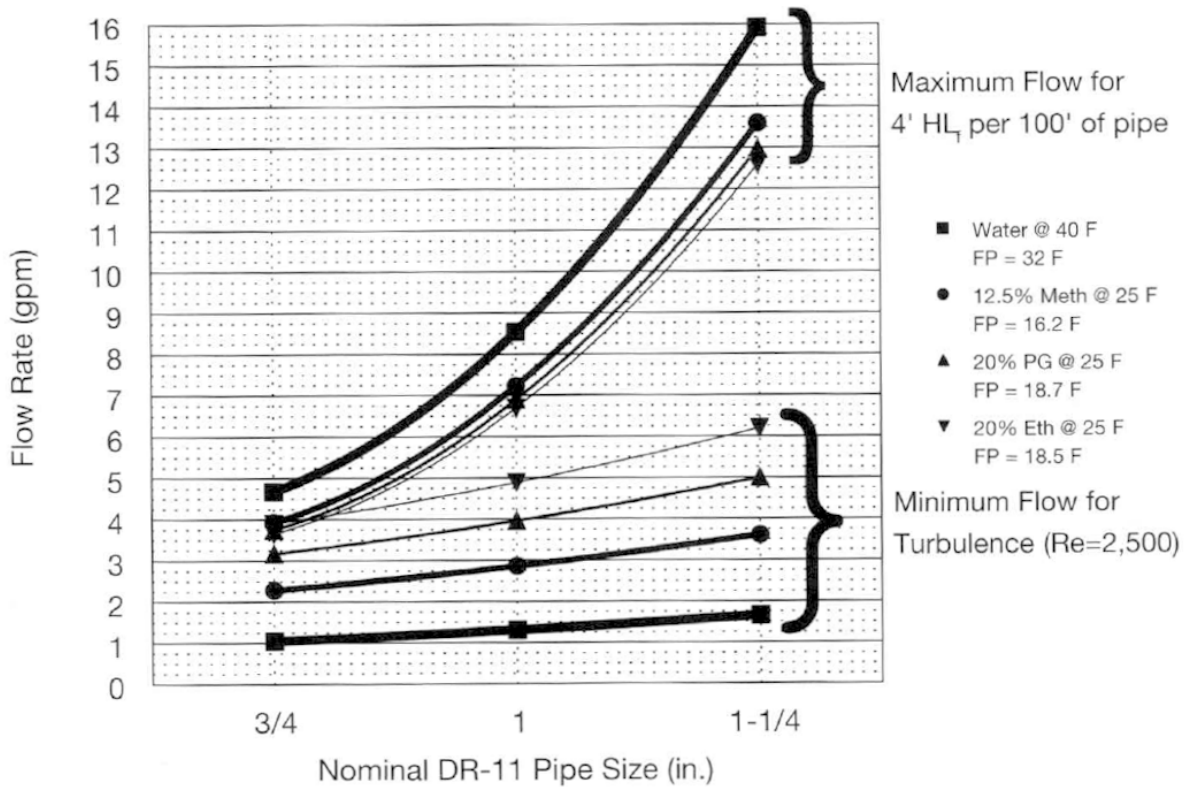
Another important design criterion related to the choice of antifreeze is the minimum temperature of the heat transfer fluid entering the heat pump. This minimum entering water temperature (EWT_{min}) is a critical parameter in determining the size of the ground loop heat exchanger (GLHE) and therefore has implications for the cost of a GSHP system. It is customary to design a GSHP system so that the EWT_{min} is 32°F, which coincides with a minimum leaving water temperature (LWT_{min}) of approximately 26°F.

As a point of reference for residential GSHP systems in New York State, a recent study (NYSERDA, 2018) reported ground loop characteristics for approximately 50 sites in Upstate New York. While the median EWT and LWT are approximately 32 and 26°F, respectively, some systems exhibit much colder conditions, with minimums of 24 and 18°F, respectively. The lower values may be due to designing the system to a lower EWT_{min}, uncertainty in system characteristics (e.g., thermal conductivity, borehole thermal resistance), or flow conditions in the GLHE that inhibit heat exchange, such as nonturbulent flow.

Figure 2. Histogram of Minimum Annual Entering (EWT) and Leaving (LWT) Water Temperatures

Forty-eight GSHP sites in Upstate New York during a calendar year (data from CDH Energy, 2018).
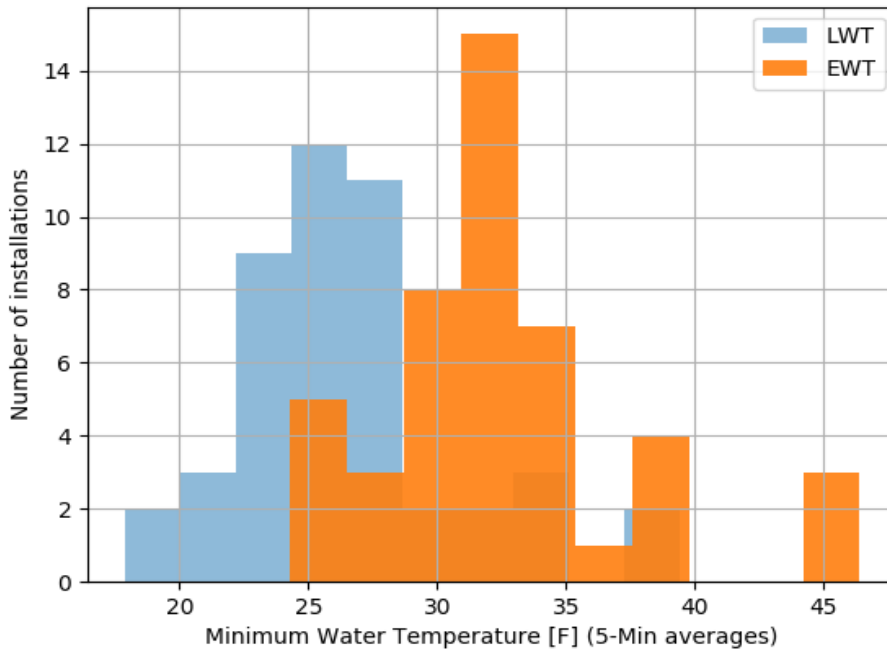
In the design of a residential or light commercial GSHP system, the thermal conductivity of the ground is often estimated using tabulated values that are representative of different rock types. The tabulated values for "average rock" and "dense rock" are 1.4 and 2.0 (Btu/hr·ft·°F) but there is little guidance as to which value is most representative for a given rock type. Clauser and Huenges (1995) report measurements on thousands of rock samples and show that, even for a given rock type (e.g., gneiss, amphibolite, clastic sedimentary, chemical sedimentary, etc.), the coefficient of variation (standard deviation divided by the mean) ranges from 15 to 50%, meaning that +/- one standard deviation represents a range of uncertainty of ±30% to 100%, respectively. Casasso and Sethi (2014) investigated the impact of uncertainty in GSHP design parameters on system performance and found that a 30% difference in thermal conductivity can impact the EWT_{min} by 4°F. They also found that if pipe spacing in a vertical single u-tube heat exchanger is the worst case, with pipes touching (IGSHPA A spacing), compared with the expected spacing (average of IGHSPA spacings B and C), EWT_{min} will be reduced by approximately 3°F. They also found that the thermal

conductivity of the grout can have a significant impact on EWT_{min}, as much as 10°F for grout conductivity of 0.6 (Btu/hr·ft·°F) compared to what they report as a typical value of 1.16 (Btu/hr·ft·°F). While it is unlikely that the worst case of the ground thermal conductivity, pipe spacing, and grout thermal conductivity will be realized in any one system, the use of antifreeze provides a critically important role to mitigate these uncertainties.

When lower water temperatures may occur, the GSHP system designer must choose an antifreeze solution that can provide greater freeze protection and maintain flow rates that provide for optimal performance (Figure 1). In the NYSERDA study (CDH Energy, 2018), 30 of the 44 closed loop systems report using methanol as the antifreeze solution. For the methanol-based systems that report a freeze protection level (n=21), 62% report a freeze protection level of 15°F or lower. When propylene glycol is used (n =14), the lowest reported freeze protection level is 20°F. From these data, it is clear that methanol is a popular choice among installers due, at least in part, to the ability to provide more freeze protection without adverse effects on system performance. In fact, six systems report a freeze protection of 10°F, indicating a recognition in the industry that actual operating conditions of the GSHP system may be quite colder than the system design. As noted, such differences may be attributed to a number of factors including, the thermal properties of the ground or ground heat exchanger may be less favorable than expected during design and lower-than expected flow rates (e.g., due to mechanical or controller problems) may adversely affect the performance of the ground loop if the flow becomes laminar.

This project characterizes the differences between propylene glycol and Kilfrost GEO at the same freeze protection levels for cold ground loop conditions that are observed but not previously considered in the literature. We then use the observed differences to evaluate the impact on system performance, system design, and system reliability. Collectively, improved performance and reliability as well as opportunities to lower installation costs will help to increase the adoption of GSHP technology and reduce the energy use of NYS consumers.

2   Methods

2.1   Experimental Apparatus

The contrast in performance of the two antifreeze solutions (Kilfrost GEO & propylene glycol) was observed in a controlled environment at Hudson Valley Community College TEC-SMART laboratories. The TEC-SMART Geothermal Lab has a closed vertical borehole heat exchanger and several heat pumps that can be mixed and matched for educational purposes. For this study, the team added a WaterFurnace 7 Series 3-ton heat pump (Model Number NVV036) and built a simulated above-ground ground loop (Figure 3). The team could then closely control a range of temperatures in the loop (15 to 35°F) over a relatively short period of time (hours).

The antifreeze solutions were circulated through a 900-foot simulated above-ground ground loop (SAGGL) that consisted of two 450 coils of 1¼ inch DR-11 HDPE pipe (Figure 4). Because the primary source of heat to the SAGGL was the room air, operating the heat pump could efficiently cool the fluid in the loop from room temperature to the upper limit of the temperature range of interest (35°F) within approximately one hour.

Experimental runs for the two antifreeze solutions were monitored using a dedicated set of calibrated sensors attached to a web-connected data acquisition system (DAQ) recording temperatures, circulator pumping energy, heat pump compressor power, fluid pressures, and fluid flow rate (Figure 5). Additional data logging was accomplished with the WaterFurnace Symphony monitoring system installed in the 7 Series heat pump.

The experimental objective was to maintain a steady temperature distribution throughout the system for approximately 10 minutes at each target EWT of 35, 30, 25, and 20°F. To achieve this stabilization of the SAGGL temperatures, it was necessary to either modulate the heat pump speed, so that heat of extraction equaled the heat gain from the room air, or to inject heat into the loop at what would normally be the u-bend. In the experimental design, it was difficult to predict the rate of heat gain from the air and the ability of the heat pump to modulate accordingly. Because a source of heat was readily available with the actual ground loop serving the TEC-SMART Geothermal Lab, we opted to put a plate heat exchanger in place of a u-bend and modulate the heat input by controlling the flow from the actual ground loop to the plate heat exchanger.

Figure 3. Photograph of Experimental Apparatus in the TEC-SMART Geothermal Lab

Figure 4. Photograph of Simulated Above-Ground Ground-Loop (SAGGL)
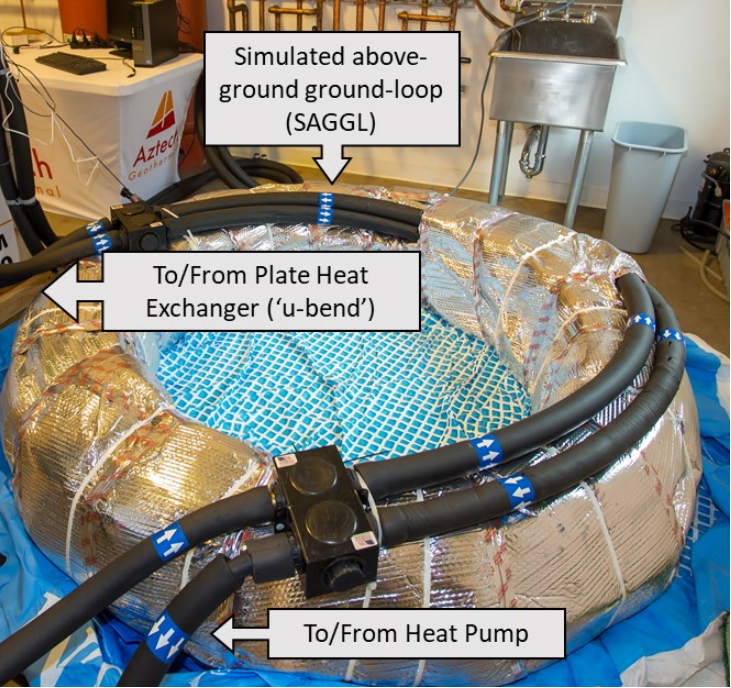
Figure 5. Schematic of Laboratory Apparatus. Connections to Data Collection Equipment and Expansion Tank Not Shown

TS - Surface mount temperature
TW - Thermal well
FM - Flow meter
PT - Pressure transducer
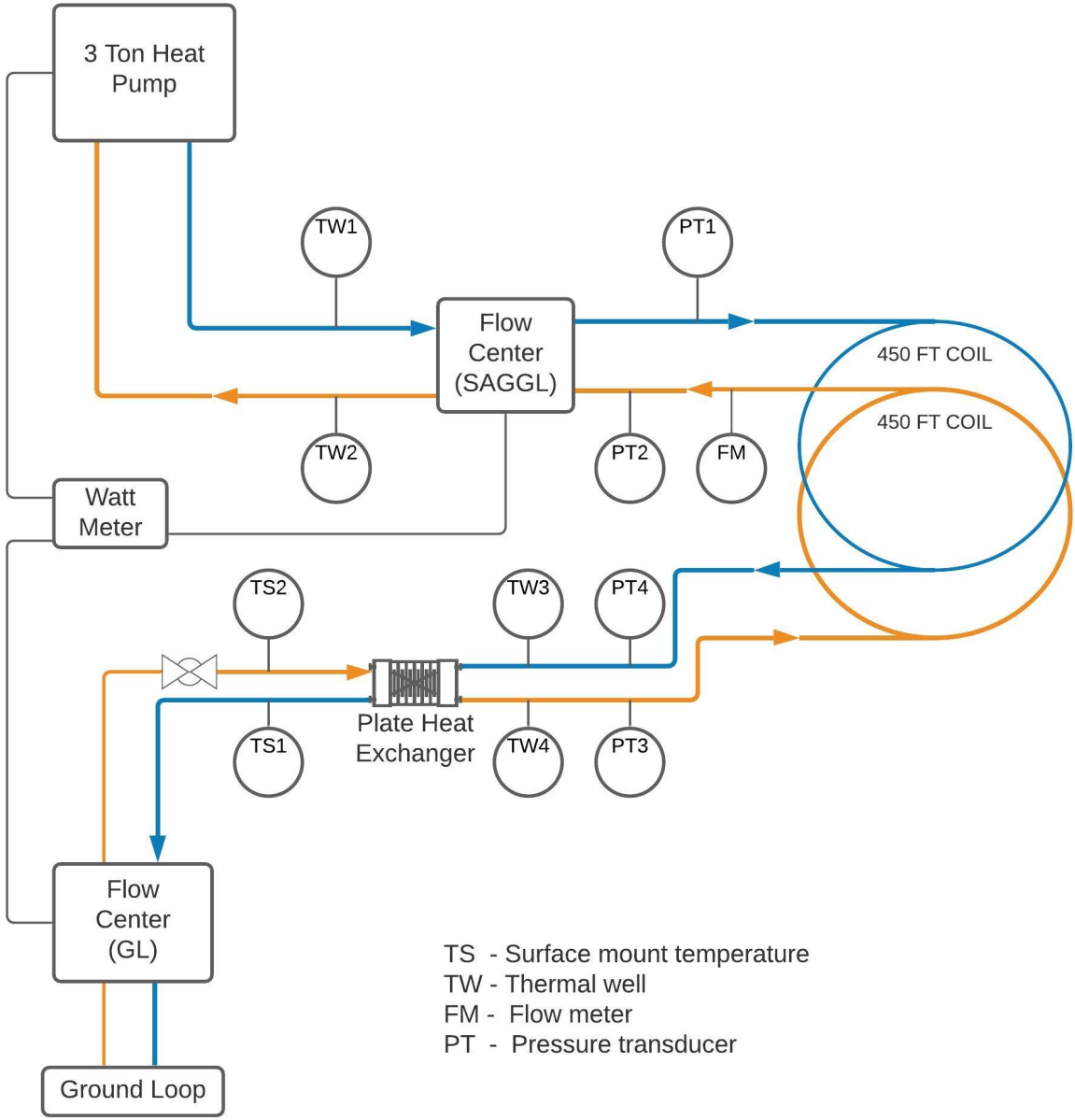
Figure 6. Annotated Photograph of SAGGL Instrumentation Panel

Refer to Table 1 for sensor labels.

Figure 7. Annotated Photograph of Ground Loop Instrumentation Panel

Refer to Table 1 for sensor labels.
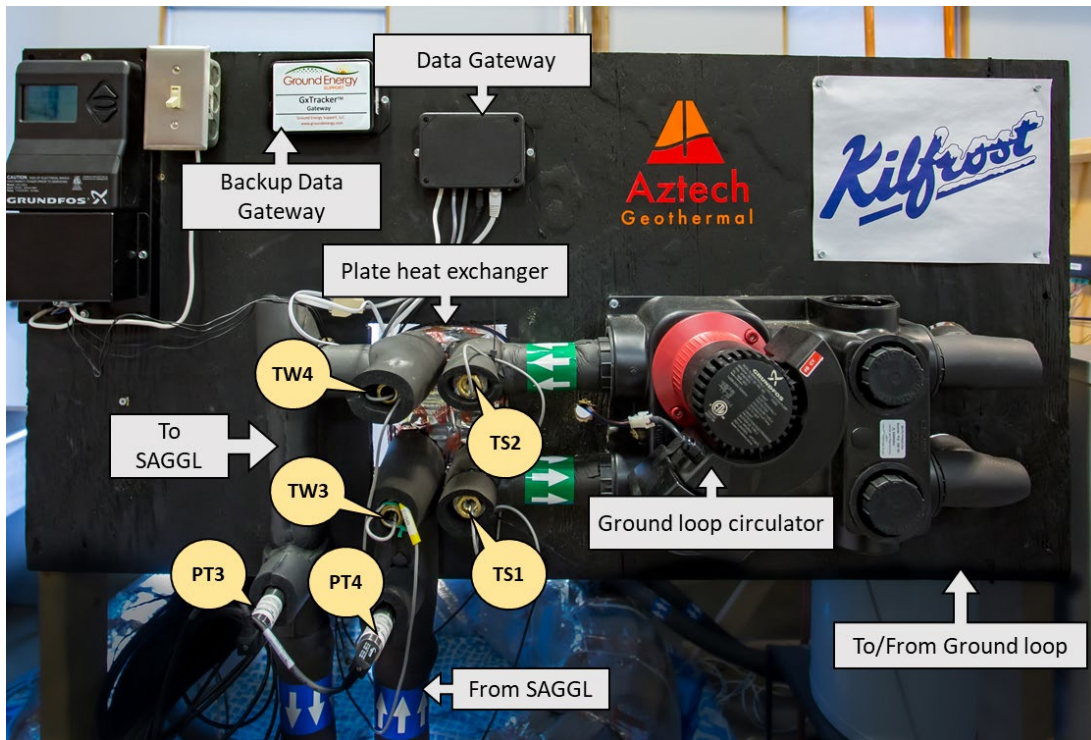
2.2 Data Collection

Data collection was accomplished using two separate data acquisition (DAQ) systems. The primary DAQ is a web-connected system that uses the GxTracker gateway to poll sensors on a 1-Wire® network and push data to a remote host for processing and storage. For temperature measurements, direct digital readings of temperature are corrected to a laboratory standard (appendix A). Other measurements are collected using analog-to-digital conversion and computed from equations provided by the device manufacturer. Measurements obtained with the primary DAQ are summarized in Table 1.

Table 1. Summary of Measurements, Devices, and Accuracy for Sensors Connected to the Primary Data Acquisition System

See Figures 5, 6, and 7 for sensor locations and photographs of control panels.

Location	Measurement	Device	Model Number	Accuracy
Heat pump (TW2)	Temperature	1-Wire temperature	Maxim DS18B20	0.05 °Fa
Heat pump (TW1)	Temperature	1-Wire temperature	Maxim DS18B20	0.05 °F
Heat exchanger (TW3)	Temperature	1-Wire temperature	Maxim DS18B20	0.05 °F
Heat exchanger (TW4)	Temperature	1-Wire temperature	Maxim DS18B20	0.05 °F
Ground loop (TS1)	Temperature	1-Wire temperature	Maxim DS18B20	0.05 °F
Ground loop (TS2)	Temperature	1-Wire temperature	Maxim DS18B20	0.05 °F
SAGGL (FM)	Fluid flow rate	Insertion turbine	Onicon F-1100	1% reading
Below circulator, entering SAGGL (PT1)	Fluid pressure	Pressure transducer (0-50 psig)	Transducers Direct TD1000	0.125 psi
Leaving SAGGL, entering heat pump (PT2)	Fluid pressure	Pressure transducer (0-25 psig)	Transducers Direct TD1000	0.063 psi
Leaving plate heat exchanger (PT3)	Fluid pressure	Pressure transducer (0-25 psig)	Transducers Direct TD1000	0.063 psi
Entering plate heat exchanger (PT4)	Fluid pressure	Pressure transducer (0-25 psig)	Transducers Direct TD1000	0.063 psi
Heat pump (W1)	Electricity use	Watt meter	WattNode WNB-3D-240-P	0.5% reading
SAGGL pump (W2)	Electricity use	Watt meter	WattNode WNB-3D-240-P	0.5% reading
Ground loop pump (W3)	Electricity use	Watt meter	WattNode WNB-3D-240-P	0.5% reading

[a]   Temperature accuracy is reported relative to the laboratory standard used for calibration that has an absolute accuracy of 0.125 °F, see appendix A for calibration description.

The WaterFurnace Symphony system (Symphony) installed in the heat pump was used to supplement the GxTracker system. The Symphony provides several important and complementary data points and is a powerful tool for monitoring the performance and accessing controls remotely for a large number of heat pumps. For both the Symphony and GxTracker, the sample interval was set to 10 seconds.

Upon completed construction of the experimental apparatus and installation of measurement equipment, a set of initial tests were conducted to identify issues in the operation of the equipment and the data collection process. Minor changes were made to the system, such as replacing pressure transducer PT1 with one with a transducer that has a higher measurement limit, as the maximum pressure exceeded 25 pounds per square inch gauge (psig). A larger expansion tank was installed to decrease the magnitude of pressure increase during the cooling of the SAGGL (and contraction of the HDPE). Calibration of the sensors was confirmed by comparing with independent measures from the Symphony system and handheld meters.

2.3 Experimental Procedure

For each experiment, the antifreeze solution was loaded into the SAGGL, and a sample of fluid obtained to confirm freeze protection level using a field refractometer and retained for laboratory analysis. The SAGGL circulating pumps were set to maintain the desired flow rate of 8 gallons per minute, and the heat pump was manually set to run at full load in heating mode. As heat was extracted from the SAGGL, the EWT was monitored continuously and the heat and the rate of flow from the ground loop into the plate heat exchanger was controlled manually with a ball valve. As the EWT approached the first temperature of interest (32°F), the heat input into the plate heat exchanger was increased slightly to maintain steady loop temperatures in the SAGGL. These quasi-steady conditions were maintained for at least 10 minutes and then the flow into the plate heat exchanger was reduced to allow the SAGGL temperature to continue to fall. As the heat pump EWT reached each successive target, the flow into the plate exchanger was again increased slightly to maintain steady temperatures. Each experiment was run until a freeze protection fault was triggered by the Symphony system recording a temperature less than 20°F for a duration of 60 seconds, shutting off the heat pump compressor. Each experimental run lasted approximately four hours.

2.4 Data Management

Each experimental run was conducted by Aztech Geothermal personnel with an antifreeze solution that was noted as either Antifreeze 1 or Antifreeze 2 so that the data analyst (Ground Energy Support) could evaluate the results without bias. Upon completion of the task and analysis of the data, the datafiles and summary report were provided to the NYSERDA Project Manager. By memorializing the data and analysis as the project progressed, the final analysis could be conducted after the identities were revealed, so that the respective fluid properties could be used to interpret the observations.

2.5 Data Analysis

For each experimental run, raw data collected from sensors was processed with calibration and offset factors. These include conversion of pulses from WattNode devices into watts over a period between samples, application of temperature calibration corrections (appendix A), addition of elevation head for pressures sensors, and calculation of flow rates from flow meter calibration parameters provided by the manufacturer.

Exploratory data analysis was conducted by generating a consistent set of time series plots for each of the experimental trials. From these observations, data were grouped into representative subsets for target temperatures by selecting intervals of approximately 10-minutes each in which the loop temperatures at the heat pump and plate heat exchanger were relatively constant. The 10-second interval data were then upscaled to 1-minute mean values resulting in approximately 10 values for each target interval. Each upscaled value within a target temperature interval is treated as a replicate for that interval.

Statistical analyses of the upscaled samples are conducted using ordinary least squares linear regression in the python package *statsmodels* (Seabold and Perktold, 2010) to identify correlations between the following combinations of variables: Pressure drop versus loop temperature; pumping power versus loop temperature; and pumping power versus pressure drop. For evaluating the significance of differences between regression parameters, the nonparametric Kruskal-Wallis test from the SciPy Statistics package is used.[1]

3 Results

3.1 Overview of Test Results

The comparison between propylene glycol and Kilfrost GEO focuses on the results of Task 5 (propylene glycol) and Task 8 (Kilfrost GEO). Task 10 (propylene glycol) was conducted as blind replicate to assess repeatability of the experimental apparatus and procedures. The results of the replicate run (Task 10) are included in appendix B.

3.1.1 Freeze Protection Levels

For each field trial, the level of freeze protection in the SAGGL was determined using field refractometers, one calibrated for propylene glycol and one calibrated for Kilfrost GEO. In addition, samples of each fluid were sent to Kilfrost for laboratory analysis with both digital refractometer and differential scanning calorimetry, results of the field refractometer and the lab tests are summarized in Table 2.

Table 2. Freeze Protection Temperatures for Experimental Runs

	Freeze Protection [°F]	
	Field Refractometer	**Lab Tests**
Propylene Glycol (Task 5)	14.0	15.8
Kilfrost GEO (Task 8)	14.0	15.3
Propylene Glycol (Task 10) [Repeat of Task 5]	14.5	17.2

The difference between field refractometer values and lab measured data can be attributed to organic acid inhibitors that affect refractive index measured with field devices, the accuracy of field refractometers ($\pm$ 0.002), compared to that of a digital refractometer ($\pm$ 0.0001), and compensation for actual fluid temperature.

3.1.2 SAGGL Flow Rates

Power to the circulating pump was modulated to maintain a constant flow rate through the duration of the test. The real-time display of the Symphony monitoring system was used to maintain the target flow rate and the Onicon meter is used as the more accurate measure of flow rate. The nominal target flow rate for each test was 8.0 gallons per minute. Because of the discrepancy between the Symphony system and the Onicon F-1100 flow meter, it was determined that the Symphony flow rate needed to be approximately 10.5 gpm to maintain a flow rate of 8 gpm, as measured with Onicon meter.

Figure 8. Comparison of Minute-Averaged Flow Rates During Test Intervals
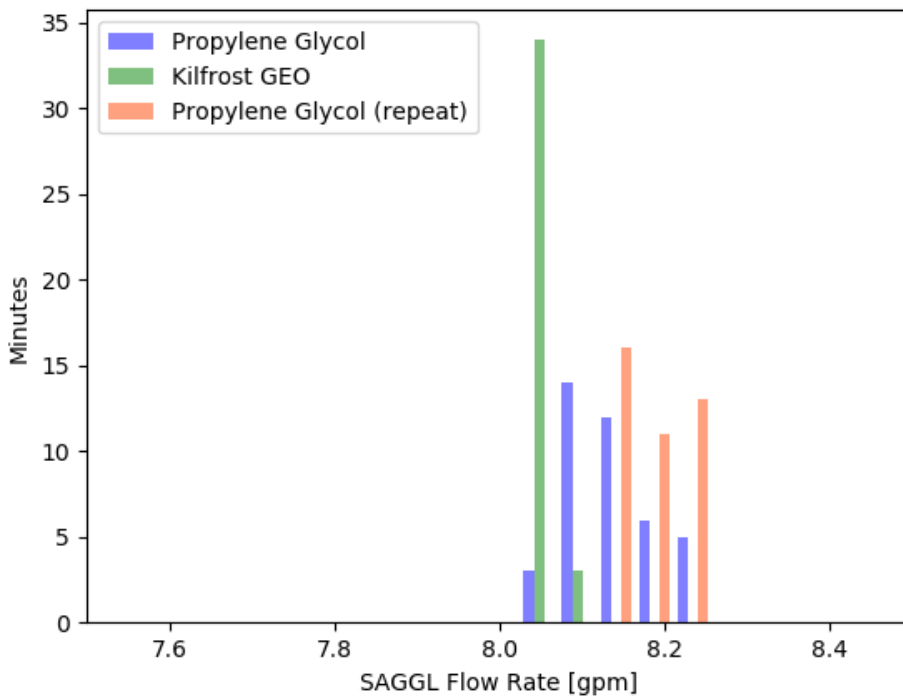
While each test was able to maintain a relatively constant pumping rate of 8.1 gallons per minute, the actual flow rates between tests did vary slightly (Figure 8). A nonparametric Kruskal-Wallis test on the flow rates for each test suggests that the null hypothesis that all have the same median values can be rejected (p-values < 1e-4). Pairwise tests also indicate that each test has a statistically distinct median flow rate. With that said, the small differences in flow rates (approximately 1.5%) are not expected to have a material effect on the experimental results or conclusions.

Table 3. Flow Rate Statistics for Experimental Runs

Test	Onicon Meter		Symphony Sensor	
	Mean Flow Rate [gpm]	Standard Devlopment [gpm]	Mean Flow Rate [gpm]	Standard Development [gpm]
Propylene Glycol (Task 5)	8.14	0.050	10.63	0.092
Kilfrost GEO (Task 8)	8.05	0.014	10.51	0.020
Propylene Glycol (Task 10)	8.18	0.036	10.70	0.080

To confirm the differences in flow between runs, flow measurements from the Symphony system were also analyzed for comparison. As shown in Table 3, the Symphony-measured flow shows the same trends in differences between runs, though a consistent bias of 2.5 gpm when compared to the Onicon flow meter.

3.1.3 Experimental Results

As described in section 2.3, each experimental trial was conducted over a period of approximately four hours. Figures 9 and 10 summarize the conditions in the SAGGL for the propylene glycol (Task 5) and Kilfrost GEO (Task 10) experimental trials, respectively. It took about one hour for the SAGGL to cool to the first target EWT of 35°F, then about 30 minutes to progress through each additional target. The 10-minute intervals for each target temperature are shown in the figures with a vertical dotted line at the beginning of the interval and a vertical dashed line at the end of the interval. Data collected during these successive quasi steady state intervals is the focus of the analysis.

As illustrated by the heat pump compressor power, the propylene glycol run experienced temporary shutdowns of the compressor at 30-minute intervals. This was due to the operation of the heat pump at full load in manual mode that times out after 30 minutes. At each shutdown, the heat pump was reset to run at full load and the SAGGL recovered prior to reaching the next target interval. In the Kilfrost GEO run (Figure 10), there was one compressor shut off as the system before reaching the first target interval and then the technician reset the control prior to the 30-minute time out.

In the propylene glycol run, the static pressure was reduced early in the run (time stamp at approximately 10:30) and again shortly after 11:30. The cooling of the propylene glycol tended to increase the fluid pressure in the loop, either due to a slight expansion of the fluid volume or a contraction of the high density polyethylene (HDPE) as it cooled. This was not observed in the Kilfrost GEO run.

Figure 9. Time Series Plot of Results with Propylene Glycol

Dotted and dashed vertical lines indicate beginning and end of target temperature interval, respectively (Task 5).
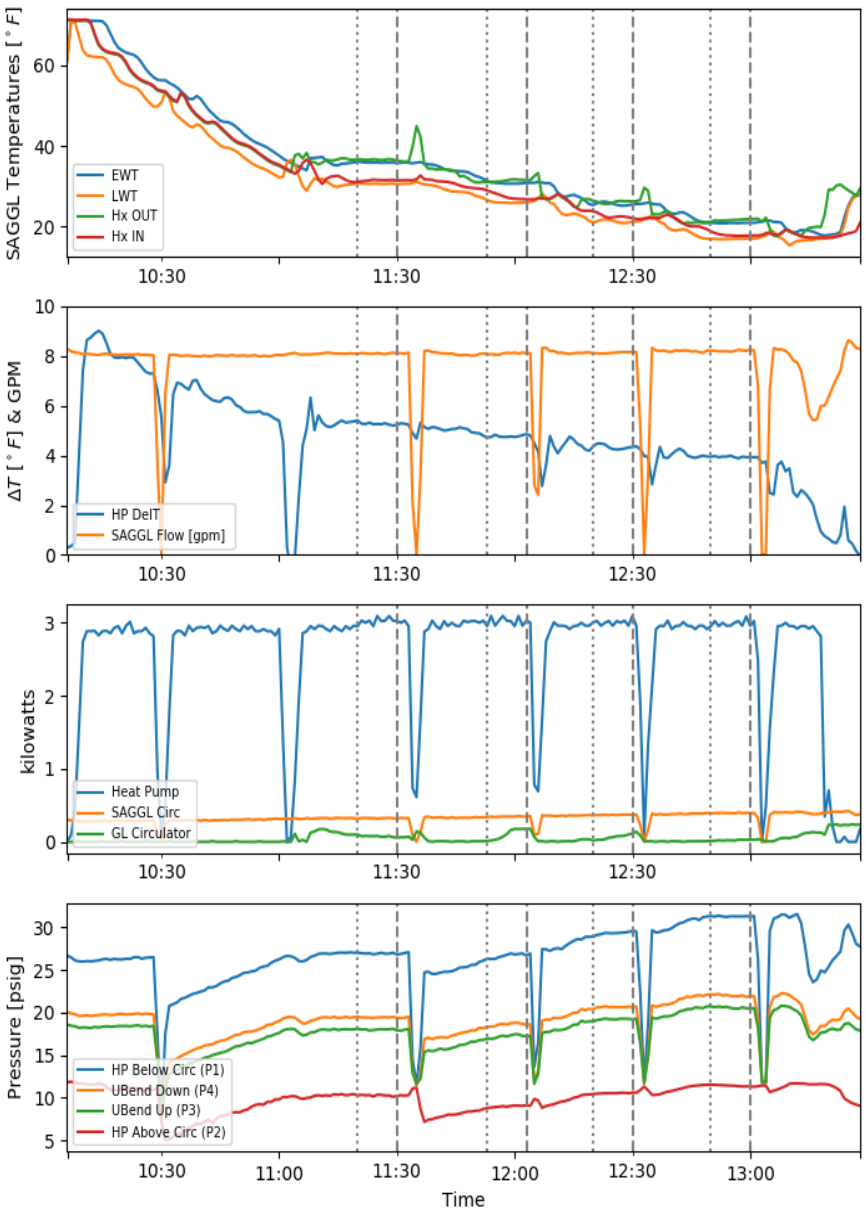
Figure 10. Time Series Plot of Results with Kilfrost GEO

Dotted and dashed vertical lines indicate beginning and end of target temperature interval, respectively (Task 10).
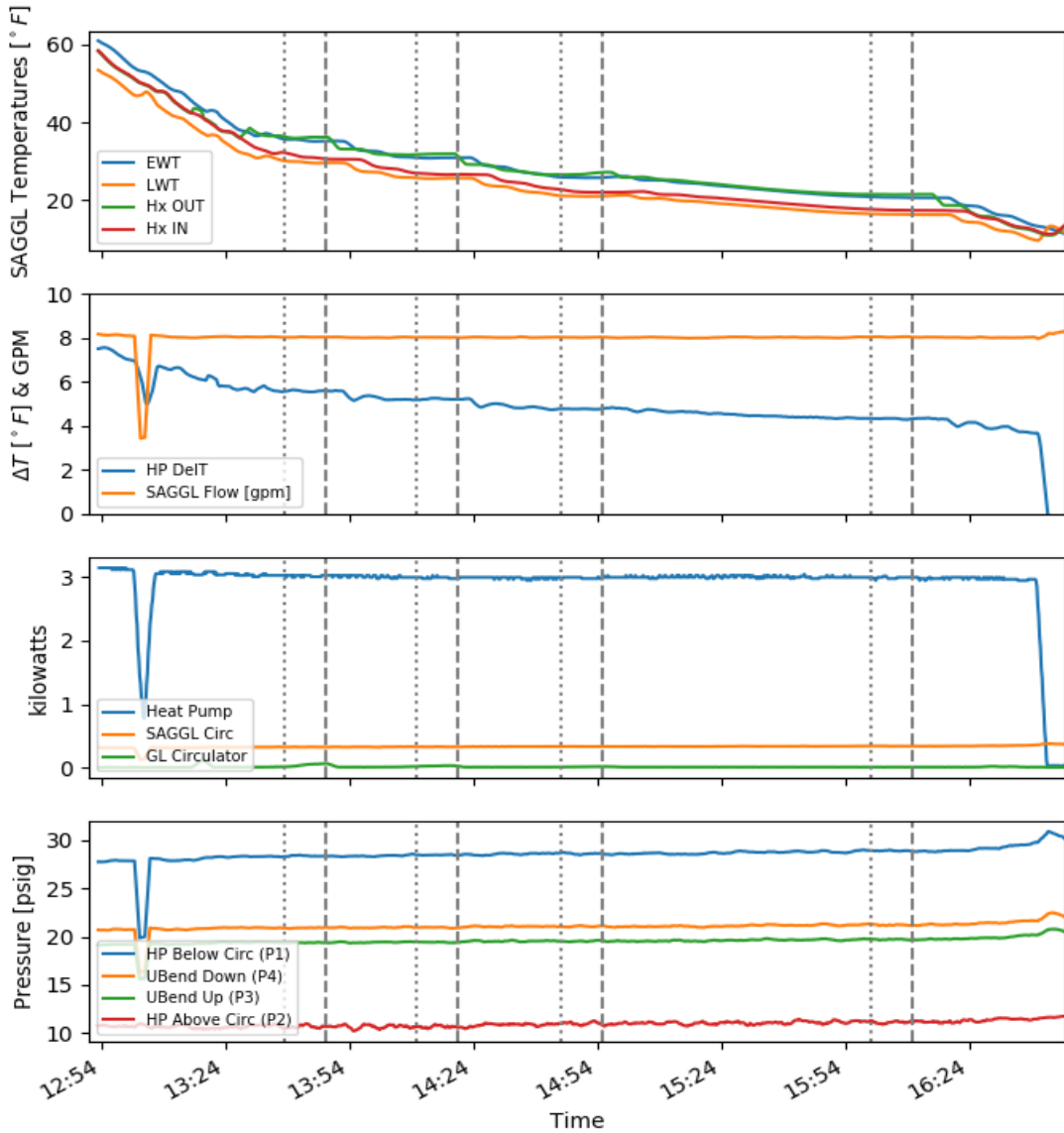
For each experimental trial, the heat pump was run until the heat pump shut off due to the freeze protection sensor. As discussed further below, the propylene glycol solution did exhibit signs of freezing as the SAGGL flow rate declined significantly prior to the heat pump shutting off, while the Kilfrost GEO solution did not.

3.1.4 Summary of Statistical Correlations

The objective of the experimental trials was to observe the behavior of the two antifreeze solutions under the same set of operating conditions and to evaluate differences in pressure drop and pumping power. The experimental design used materials commonly used in GSHP installations and evaluated behavior at the colder end of typical temperatures observed in a GSHP installation. In the evaluation of statistical relationships, the measured pressure drop, including the small change in hydrostatic pressure, is used as the measure of pipe losses.

The objectives of the statistical analyses are to determine correlations that are statistically significant and use the estimated parameters to develop an empirical relationship between variables. Here, we use ordinary least squares regression on a linear model ($y = mx + b$) and evaluate statistical significance relative to the rejection of the null hypothesis that the slope is equal to zero ($P < 0.05$).

3.1.4.1 Pressure Drop versus Fluid Temperature

We hypothesized an inverse correlation between pressure drop in the SAGGL and the mean loop temperature because as viscosity increases with colder temperatures a greater pressure drop is required to maintain the constant flow rate. This correlation is observed for propylene glycol but not for Kilfrost GEO (Figure 11). As discussed in detail in the results section, Kilfrost GEO exhibits a smaller change in viscosity over the temperature range considered, resulting in no significant increase in pressure drop. The lower pressure drop for propylene glycol at temperatures greater than 32°F, is attributed to the Kilfrost GEO flow remaining turbulent while the propylene glycol flow is laminar. This too is discussed in more detail in section 3.2.1 Modeling of Experimental Observations.

Figure 11. Pressure Drop in SAGGL as a Function of Average Loop Temperature

Regression line is plotted for propylene glycol. Kilfrost GEO does not exhibit a statistically significant correlation.
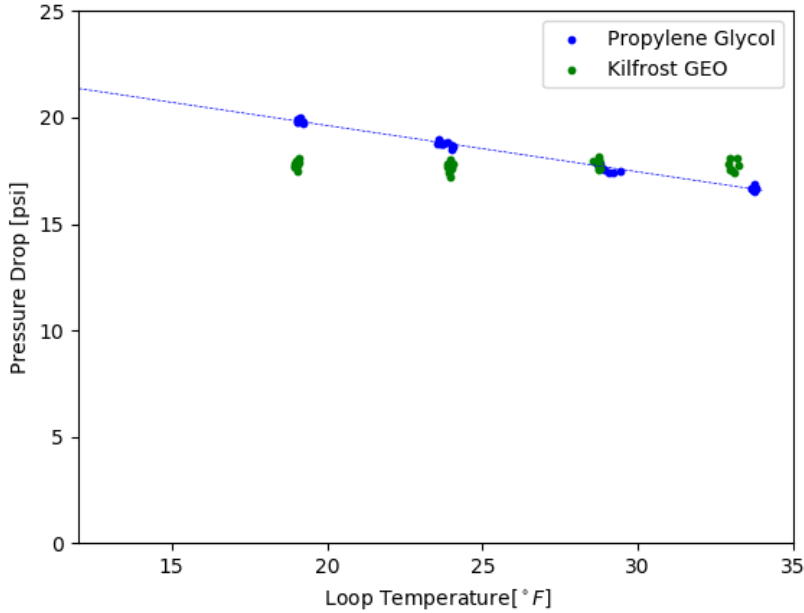
Table 4 summarizes the statistical relationship for propylene glycol, which has a statistically significant negative slope. The Kilfrost GEO solution does not have a slope that is statistically different from zero (Table 5).

Table 4. Regression Statistics for Pressure Drop versus Loop Temperature, Propylene Glycol

No. Observations		40		R-squared		0.992
Df Residuals		38		F-statistic		4504.
Df Model		1		Prob (F-statistic)		4.36e-41
coefficient		Std err	t	P>|t|	$CI_{0.025}$	$CI_{0.975}$
Intercept	23.830	0.087	272.753	0.000	23.652	24.006
Slope	-0.218	0.003	--67.111	0.000	-0.224	-0.221

Table 5. Regression Statistics for Pressure Drop versus Loop Temperature, Kilfrost GEO

No. Observations			37		R-squared		0.000
Df Residuals			35		F-statistic		1.671e-06
Df Model			1		Prob (F-statistic)		0.999
coefficient		Std err		t	P>|t|	$CI_{0.025}$	$CI_{0.975}$
Intercept	17.609	0.194		90.864	0.000	17.215	18.002
Slope	-9.59e-6	0.007		-0.001	0.999	-0.015	0.015

3.1.4.2 Pumping Power versus Pressure Drop

The greater head loss (pressure drop) necessary to maintain a constant flow rate is manifested through a greater power required by the SAGGL circulating pumps. As shown in Figure 12 and Tables 6 and 7, the measurable increase in pressure drop for propylene glycol also results in a measurable increase in pumping power. For Kilfrost GEO, there is not a statistically significant increase in the pressure drop required to maintain a constant flow rate and likewise there is not a statistically significant increase in pumping power. Because the cluster of points for Kilfrost GEO (Figure 12) are close to the line for propylene glycol, we can use the observed relationship for propylene glycol as a general empirical relationship between pumping power and pressure drop for the temperatures and viscosity ranges in the experimental trials.

Figure 12. Pumping Power as a Function of Pressure Drop in SAGGL

Regression line is plotted for propylene glycol. Kilfrost GEO does not exhibit a statistically significant correlation.
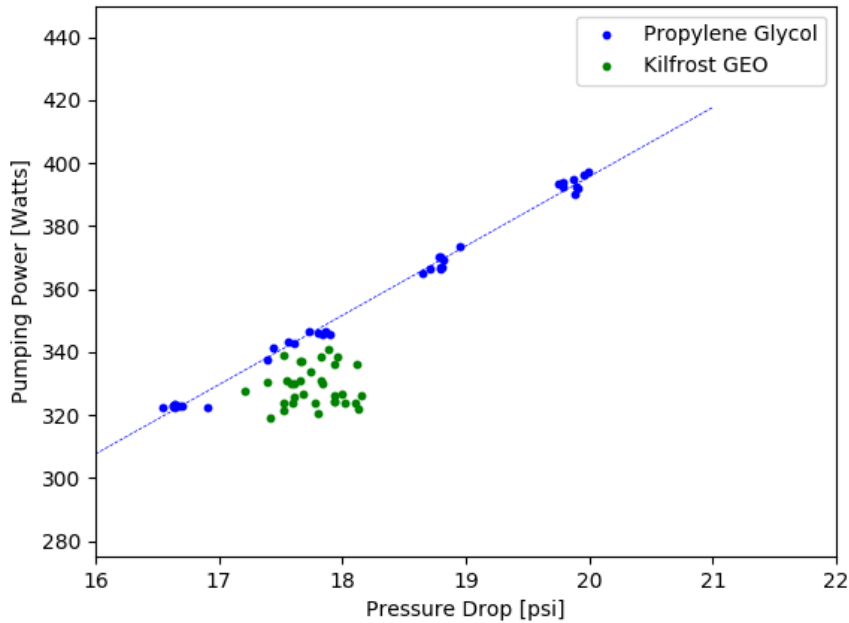
Table 6. Regression Statistics for Pumping Power versus Pressure Drop, Propylene Glycol

No. Observations			36		R-squared		0.994
Df Residuals			34		F-statistic		4674.
Df Model			1		Prob (F-statistic)		2.04e-39
coefficient		Std err		t	P>|t|	$CI_{0.025}$	$CI_{0.975}$
Intercept	-41.270	5.302		-8.338	0.000	--52.044	-30.495
Slope	22.0140	0.292		75.328	0.000	21.420	22.608

Table 7. Regression Statistics for Pumping Power versus Pressure Drop, Kilfrost GEO

No. Observations		33		R-squared		0.001
Df Residuals		31		F-statistic		0.01931
Df Model		1		Prob (F-statistic)		0.890
coefficient		Std err	t	P>|t|	$CI_{0.025}$	$CI_{0.975}$
Intercept	317.851	81.516	3.899	0.001	151.599	484.104
Slope	0.6431	4.628	0.139	0.890	-8.796	10.083

3.1.4.3 Pumping Power versus Fluid Temperature

While the results did not detect a statistically significant correlation between either pressure drop and loop temperature or pumping power and pressure drop for Kilfrost GEO, a statistically significant correlation between pumping power and fluid temperature was observed for both propylene glycol and Kilfrost GEO (Figure 13). Consistent with the lack of correlations between some variables, the correlation between pumping power and fluid temperature for Kilfrost GEO has a small, but not negligible slope. The reason for a correlation with this pair of variables is attributed to the large variation in temperatures, rather than a large variation in pumping power.

Figure 13. Pumping Power as a Function of Loop Temperature in SAGGL

Regression lines are plotted for both propylene glycol and Kilfrost GEO.
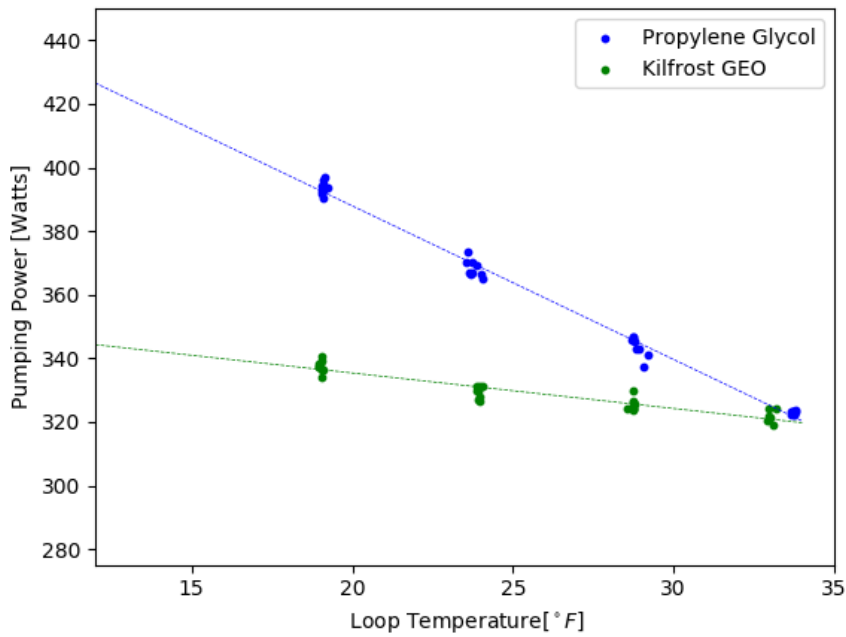
Table 8. Regression Statistics for Pumping Power versus Loop Temperature, Propylene Glycol

No. Observations		36		R-squared		0.992
Df Residuals		34		F-statistic		4389.
Df Model		1		Prob (F-statistic)		1.56e-37
coefficient		Std err		t	P>|t|	$CI_{0.025}$	$CI_{0.975}$
Intercept	484.535	7.963		246.849	0.000	480.546	488.524
Slope	-4.830	0.073		-66.250	0.000	-4.978	-4.682

Table 9. Regression Statistics for Pumping Power versus Loop Temperature, Kilfrost GEO

No. Observations			33		R-squared		0.876
Df Residuals			31		F-statistic		218.4.
Df Model			1		Prob (F-statistic)		1.39e-15
coefficient		Std err		t	P>|t|	CI$_{0.025}$	CI$_{0.975}$
Intercept	357.691	1.966		181.917	0.000	353.680	361.701
Slope	-1.116	0.075		-14.779	0.000	-1.270	-0.962

3.1.5 Differences in Fluid Flow at Low Temperatures

Each test was run until the heat pump shut down due to a freeze protection (FP) fault code in the WaterFurnace controls. The FP fault is triggered when the FP1 sensor records temperatures less than 20°F for a duration of 60 seconds. Because the FP level is hard coded, it is not a good indicator of when loop fluid actually begins to freeze. Instead, we interpret the time when the flow rate begins to decline as the first sign of fluid freezing.

Figure 14. Comparison of Symphony Measurement at the End of Experiment for Propylene Glycol and Kilfrost GEO

Horizontal dotted lines represent laboratory freeze protection values from Table 2 and Symphony flow rate. Time range for each is 12 minutes.
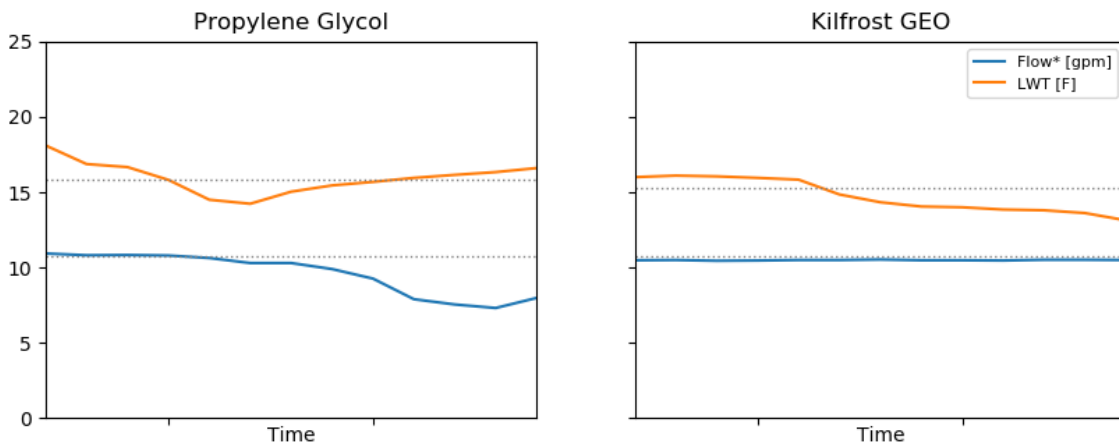
As shown in Figure 14, the flow rate for propylene glycol begins to decline when the water temperature leaving the heat pump (LWT) drops below the freeze protection level. The flow rate continues to decline indicating continued freezing. Kilfrost GEO, on the other hand, shows no signs of freezing, even when the fluid temperature drops well below the measured freeze point.

We hypothesize that the difference in behavior is attributed to propylene glycol being in the laminar flow regime (as discussed in the 3.2.1 Modeling of Experimental Observations section) while Kilfrost GEO is turbulent. Under turbulent flow, fluids have been observed to become "supercooled" and remain in the liquid state below their freeze point. Arora and Howell (1973) envision a distance from the tube wall at which the fluid temperature must be at or below the freeze point in order for ice to form. For freezing to occur, the turbulent boundary layer must be larger than "a minimum critical molecular chain length ... or some other microscopic phenomenon" to allow for ice to form. If the turbulent boundary layer is less than this distance, the crystals will not be nucleated. For the experiments conducted here, the flow for propylene glycol is laminar for all flow conditions due to higher viscosity so there is nothing to inhibit the formation of ice at supercooled temperatures.

3.2   Flow Conditions in the SAGGL

The experimental design focused on the ability to evaluate differences based solely on empirical observations. Unfortunately, the experimental design did not account for the effects of the coiled pipe (Figure 5) or the impact of changes in fluid viscosity would have on the flow regime in the SAGGL. A deeper investigation into these differences was led by the somewhat surprising observation that the differences in pressure drop between the antifreeze solutions was small and (Figure 11) and, in fact, Kilfrost GEO exhibited greater pressure drop at the 35°F temperature. To characterize the flow conditions in the SAGGL, it is necessary to quantify (1) the Reynolds number, accounting for changes in viscosity with temperature and (2) the effect of the 900 ft of coiled pipe, which is characterized by the Dean number.

The Reynolds number is a fundamental dimensionless parameter that measures the relative strengths of inertial forces (mass times velocity) to viscous forces and is commonly used to determine whether flow is turbulent or laminar. The Reynolds number (Re) is defined as:

$$Re = \rho v d / \mu$$

And where ρ is the fluid density, v is the average axial velocity, and μ is the dynamic viscosity. When viscous forces dominate and Reynolds numbers are low, flow is laminar and pressure loss calculations are relatively straightforward as f is inversely proportional to Re. When, on the other hand, inertial forces dominate, flow in the pipe becomes turbulent. Generally, turbulent flow is preferred for heat transfer as fluid is well mixed in the pipe. Under laminar flow conditions, the fluid along the boundary tends to equilibrate with the temperature outside of the pipe impeding thermal exchange with fluid temperatures near the center of the pipe.

Figure 15. Comparison of Viscosity as a Function of Temperature

Values computed from viscosity model provided by Kilfrost.
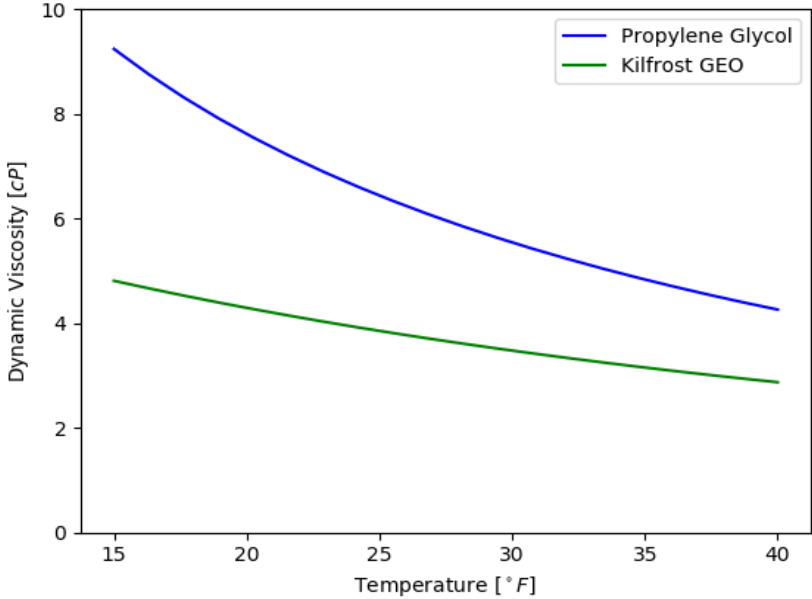
To calculate the Reynolds numbers over the range of experimental conditions, we used a viscosity model developed by Kilfrost that was developed for both propylene glycol and Kilfrost GEO. This enables the calculation of fluid viscosities over a range of temperatures and freeze protection levels. The Viscosity Model is based on experimental observations and consists of a multidimensional fifth-order polynomial (26 terms) with independent variables of freeze protection and fluid temperature. The fluid viscosities for the range of experimental conditions are shown in Figure 15. While the viscosity model has not been independently evaluated, the model produces values that are consistent with the experiments undertaken here as well as other published results for propylene glycol.

For the experimental conditions in this study, most of the SAGGL pipe length and pressure drop occurs in HDPE pipe that remains in coiled form as supplied by the manufacturer. The hydraulic geometry of coil is defined by the dimensionless curvature, $\lambda = d/D$, where d is the diameter of the pipe and D is the diameter of the coil. For the experimental conditions here, $\lambda = 0.027$. Due to centrifugal forces, flow in coiled pipe can result in one or two secondary flow fields referred to as Dean vortices. The presence and strength of these secondary flows is determined by the Dean number:

$$De = Re\sqrt{\lambda}.$$

For the experimental conditions here, Dean numbers range from 340 to 960 for propylene glycol and 660 to 1350 for Kilfrost GEO. Ghobadi & Muzychka (2016) note that secondary vortices are well established when Dean numbers are greater than 100. We therefore expect to see effects of Dean vortices in the experimental observations.

The Dean vortices in coiled pipe inhibit the development of turbulence relative to straight pipes. There have been numerous studies that evaluate the critical Reynolds number at which flow in coiled pipe becomes turbulent (Re_{crit}) and (Cheng et al., 2020) summarize seven of these studies. For λ in the range of those observed in our experiments, the average of Re_{crit} is 4700 and is much larger than the Reynolds number for straight pipes at which flow becomes turbulent, approximately 3000. Unlike straight pipes, there is less consensus on the transition region between laminar and turbulent flow in coiled pipe.

The Reynolds numbers for the experimental conditions in this study are summarized in Figure 16. Because the flow was maintained as constant (8 gpm), the variation in Reynolds numbers is attributed to the changes in fluid viscosity at different temperatures. Also shown in Figure 16 are the boundaries between laminar and turbulent flow for both straight pipe and coiled pipe.

The flow conditions in the SAGGL over the range of experimental conditions in this study are more complex than expected. We expected that by having the same flow rates and maintaining Reynolds numbers greater than 2000 both antifreeze solutions would remain in the turbulent flow regime. However, as shown in the statistical analysis section, we found unexpected differences in pressure drops between propylene glycol and Kilfrost GEO, particularly at temperatures greater than

32°F, where the pressure drop for Kilfrost GEO is larger than for propylene glycol even though Kilfrost GEO has a lower viscosity. Through closer inspection of the measurements, the characteristics of the experimental apparatus, and the flow and temperature ranges used, we found that propylene glycol is dominantly in the laminar flow regime while Kilfrost GEO is turbulent.

Fortunately, and somewhat fortuitously, when using the average Re_{crit} for coiled pipe (4700) combined with the flow rates and viscosity conditions, flow in the SAGGL can be considered as either turbulent (Kilfrost GEO) or laminar (propylene glycol). While there is likely a range of Reynolds numbers over which this transition occurs, as with straight pipe, for simplicity we use the average empirical Reynolds number of 4700 to differentiate between laminar and turbulent.

Figure 16. Reynolds Number Calculated for Experimental Conditions

Note that laminar and turbulent flow regime boundaries differ between coiled pipe and straight pipe. For Kilfrost GEO is turbulent except at the coldest temperatures in coiled pipe. Propylene glycol is laminar except at the warmest temperatures in straight pipes.
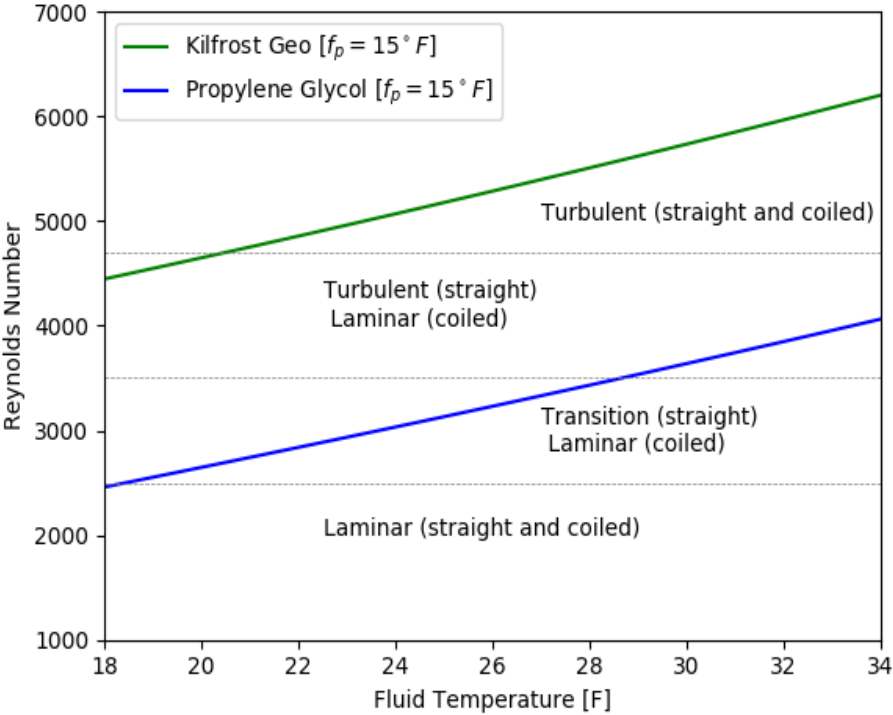
3.2.1 Modeling of Experimental Observations

The evaluation of the flow conditions in the SAGGL provides a hypothesis that flow regimes differ between the experimental runs. To evaluate this hypothesis, we quantify the effects that different flow regimes have on the pressure drop in pipe. The pressure drop in the SAGGL fluid (ΔP_f) can be calculated using the Darcy-Weisbach equation. Several forms of this equation exist. One common expression is from Fay (1994)[2]:

$$\Delta P_f = \frac{f L \rho v^2}{2 d_i}$$

Where f is the friction factor, L is the length of pipe, ρ is the fluid density, v is the fluid velocity (Q/A) and d_i is the internal diameter of the tube. The additional pressure losses due to pipe fittings is usually accounted for by adding pipe length, according to the numbers and types of fittings present. While the Darcy-Weisbach equation generally holds for all flow conditions, the formulation of the friction factor is different for laminar and turbulent flow and for straight versus coiled pipes.

Pressure drop for the experiments are calculated as the sum of pressure drops in the coiled pipe, the straight pipe along with an adjustment for fittings, the heat pump, and the plate heat exchanger (Hx).

$$\Delta P_{total} = \Delta P_{coiled} + \Delta P_{pipe/fittings} + \Delta P_{HeatPump} + \Delta P_{Hx}$$

The pressure drop through the heat pump is taken from the WaterFurnace performance data as 2.7 pounds-per-square-inch (psi) and the pressure drop through the brazed plate heat exchanger was measured consistently as 1.5 psi. Pressure drop through the straight pipe and fittings is calculated using the Darcy Weisbach equation with the Churchill friction factor using a length of 33 feet. Pressure drop in the coiled pipe is calculated with the Darcy-Weisbach equation using friction factors that account for the range of flow conditions and are described in detail in appendix C.

Figure 17. Measured (Symbols) and Modeled (Lines) Pressure Drop for Kilfrost GEO and Propylene Glycol
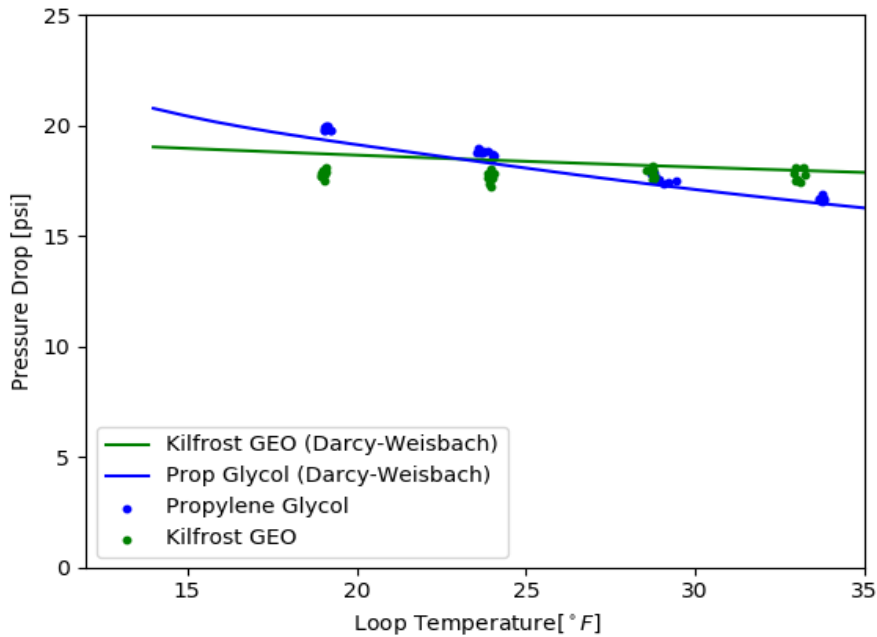
The unexpected observations of a higher pressure drop in Kilfrost GEO at temperatures greater than 28°F (Figure 17), even though it has a lower viscosity, is explained by the unique set of conditions present during the experiments. For the flow rate, pipe size chosen, pipe geometry (λ), and the range of viscosities encountered, propylene glycol remains in the laminar flow regime and exhibits a pressure drop that is approximately linearly related to temperature (and viscosity), as expected. The apparent lack of correlation between pressure drop, loop temperature (i.e., viscosity), and the higher magnitude of pressure drop for Kilfrost GEO, even though it has a lower viscosity, is attributed primarily to the Kilfrost GEO being in the turbulent flow regime for the range of conditions observed.

One of the main advantages of Kilfrost GEO over propylene glycol—when both products are at the same freeze protection level—is Kilfrost GEO's ability to maintain turbulent flow over a wide range of temperatures with minimal increase in pumping power. It is well recognized that maintaining turbulent flow in a ground loop heat exchanger is beneficial to the performance of the ground loop as the convective thermal resistance in the pipe is much lower under turbulent flow conditions. Because of the small effect that temperature has on the viscosity of Kilfrost GEO, a greater degree of freeze protection can be provided without adverse effects (such as loss of turbulent flow or need for increased pumping capacity).

4   Discussion

The team utilized the experimental results and the Darcy Weisbach calculations for straight pipe flow to quantify the potential benefits of Kilfrost GEO to improve the affordability of GSHP systems in terms of operating costs, capital costs, and the performance of GSHP systems under both normal and adverse operating conditions. While the team used software tools that are commonly used in the industry and methods from the industry and scientific literature, the analyses are limited to a set of illustrative hypothetical scenarios to illustrate the potential impacts of different antifreeze solutions under typical design and operating conditions.

4.1   System Design and Antifreeze Choice

In GSHP system design, the choice of antifreeze has two primary impacts, the ability to (1) protect the system against adverse cold conditions (reliability) and (2) provide cost effective heat energy transfer. First, the fluid must provide insurance against system malfunctioning if the ground loop were to become significantly colder than system design expectations. The choice of antifreeze is often related to a set of system design characteristics, namely flow rates, pipe sizes, and head loss in the ground heat exchanger. As illustrated in Figure 1, optimal combinations of flow rates and pipe sizes are limited according to two common constraints. While lower flow rates result in less head loss, a flow rate that is too low will result in laminar flow in the ground loop, inhibiting heat transfer with the ground.

For cost-effective heat energy transfer, the heat exchange fluid viscosity is a key factor in determining the range of optimal flows for a given pipe size. Higher viscosity fluids require a greater pumping power and add to GSHP system operating cost. Higher viscosity fluids also required a higher minimum flow to remain turbulent. Degradation of heat energy exchange under laminar flow conditions can have significant effects on system operation. Both the sources and impacts of this degradation are discussed in more detail in section 4.3 System Reliability.

Traditional choices of antifreeze often found in GSHP design software include methanol and propylene glycol. It is well established that because temperature has a smaller effect on viscosity for methanol compared to propylene glycol, the range of flows that satisfy the common design constraints are broader. This is illustrated in Figure 1 for a 25°F fluid. With respect to maintaining an optimal range for flow rate, methanol with a freeze protection of 16.2°F is clearly better than propylene glycol with a freeze protection of 18.7°F, maintaining a much larger range while also having greater freeze protection.

In the experimental trials, the team used the same freeze protection levels (15°F) for both propylene glycol and Kilfrost GEO, so that the fluids could be compared under the same experimental conditions. However, in applied settings, it is uncommon for propylene glycol to be used with a 15°F freeze protection. As noted, in a recent heat pump study in Upstate New York (CDH Energy, 2018), of the 14 installations that used propylene glycol, none had freeze protections less than 20°F. The lower-viscosity antifreezes, such as methanol and Kilfrost GEO, are commonly used at lower freeze protection levels. To capture these practices in the industry, our cost-benefit analysis compares propylene glycol at 20°F freeze protection and Kilfrost GEO at 15°F freeze protection.

While the physical properties of methanol provide advantages in system operation, methanol is also both flammable and toxic. The NYS Clean Heat program limits the concentration of methanol to 12.5% by weight due to concerns about the flashpoint of methanol, equating to a freeze protection of 16°F. In addition to its flammability, methanol is also a common antifreeze in windshield washer fluids and its toxicity at 30% is well known.

Figure 18 illustrates how different antifreeze solutions impact the design of a ground heat exchanger and follows the same approach as IGSHPA (2011). In this case, the curves are calculated using the Darcy-Weisbach equation for straight pipes and the fluid viscosities computed from an industry model provided by Kilfrost. The range of flows (shaded regions) for each solution have a lower bound that is necessary to establish turbulent flow for straight pipe and an upper bound that maintains a head loss of 4 feet per 100 feet of pipe length. Figure 18 extends the pipe size range to include one-and-a-half inch pipe. Kilfrost GEO plots very close to methanol as Kilfrost GEO also has a smaller change in viscosity at lower temperatures, compared to propylene glycol. Kilfrost GEO therefore provides the benefits of methanol—a wider range of flows with greater freeze protection—while not carrying the risks of flammability and toxicity. Our experimental results suggest that for coiled pipe, that is common in horizontal and pond loops, the higher viscosity antifreezes, like propylene glycol, require higher flow rates to remain turbulent when compared to straight pipe.

Figure 18. Flow Rate Ranges for Methanol, Propylene Glycol, and Kilfrost GEO in Straight Pipe in Comparison to Figure 1

Note that propylene glycol has a freeze protection of 20°F, compared to 15°F for methanol and Kilfrost GEO.
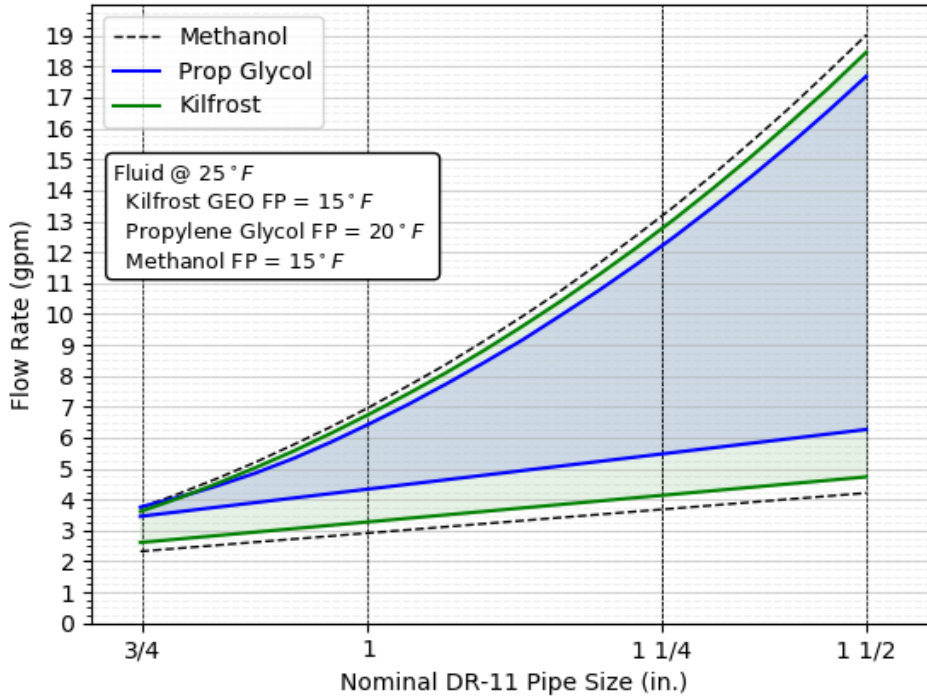
4.2   Cost-Benefit Analysis

The mathematical models arising from the experimental work conducted in this study can be used to quantify some of the potential benefits of using Kilfrost GEO. These benefits are described below in terms of either savings for pumping power, or reduced borehole drilling expenditure.

4.2.1 Pumping Power

From the NYSERDA study (CDH, 2018) all 30 sites using methanol opt for a 15°F freeze point, whereas the 14 sites using propylene glycol resulted in a 20°F freeze point or higher. This indicates that, if the antifreeze permits, a freeze point of 15°F is preferable. To compare the performance of Kilfrost GEO and propylene glycol solutions subjected to ground loop temperatures typical of the Northeast US, one year of operating data from a residential heat pump installation in southeastern New Hampshire was used to simulate pumping power and electrical demand for different conditions. As propylene glycol does not permit efficient usage at freeze points below 20°F and Kilfrost GEO is intended to be used at 15°F or less, these factors are the parameters for comparing their performance.

Figure 19. Histogram of Measured Ground Loop Temperature over a One-Year Period Used to Represent Typical Conditions

Data source: Ground Energy Support.
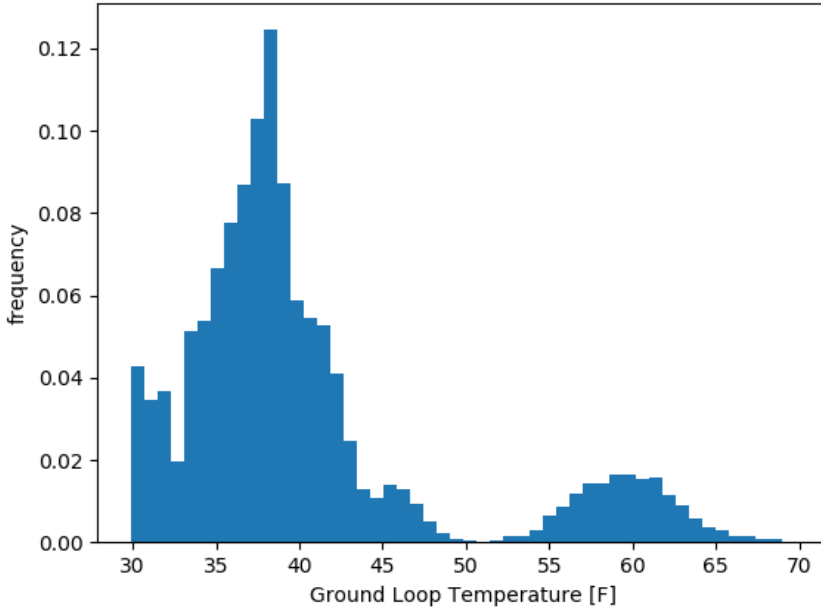
The ground loop temperature is calculated as the average of the measured entering and leaving water temperatures (Figure 19). To compute the pumping power, we use the empirical relationship between pumping power (PP) and pressure drop (ΔP) developed in the experimental trials:

$$PP = 22.01 \cdot \Delta P - 44.6$$

Where pumping power is in units of watts and pressure drop is in units of psi. The pressure drop (ΔP) is calculated using the Darcy-Weisbach equation with Reynolds numbers varying with temperature (according to the viscosity model discussed), and the Churchill model for pipe friction factor to account for the full range of Reynolds number conditions. While the flow conditions in the experimental trials were different than the conditions in the simulation here (pipe geometry and freeze protection levels), the empirical relationship observed is related to the pumping efficiency of the circulator pumps used, which are typical for GSHP installations. The empirical relationship can then be applied to other pipe geometries and freeze protection levels where the pressure drop is calculated rather than measured. The ground loop is simulated as a 650-foot vertical borehole heat exchanger with one-and-a-quarter inch DR-11 pipe with a single u-bend.

Pumping rates ranging from 8 gpm to 20 gpm are analyzed. For each temperature record, the following calculations are performed for each antifreeze solution: (1) fluid viscosity using the viscosity models described, (2) the Reynolds number, (3) the pressure drop from the Churchill equation, and (4) the pumping power from the empirical observations. Instantaneous pumping power is multiplied by the time interval of the measurement to calculate kWh, which are then summed over the year.

Table 10. Computed Pumping Power for Kilfrost GEO and Propylene Glycol at Freeze Protections of 15°F and 20°F, respectively

Flow Rate [gpm]	kWh (annual)		Kilfrost GEO Energy Savings Relative to PG-20	Max Power [W]		Kilfrost GEO Peak Reduction Relative to PG-20
	GEO-15	PG-20		GEO-15	PG-20	
8	658	702	7%	235	256	9%
12	1465	1538	5%	515	555	8%
16	2481	2611	5%	875	937	7%

Results suggest that in addition to increased freeze protection Kilfrost GEO also allows for approximately 5% savings in electricity usage. When comparing Kilfrost GEO with propylene glycol at the same 20°F freeze point, electricity savings would range from 11 to 15%. These results are consistent with the analysis of Gagné-Boisvert & Bernier (2017), where Kilfrost GEO has similar viscosity characteristics as methanol, without the inherent toxicity or flammability risks.

4.2.2 Ground Loop Temperatures in Cold Climates

In addition to the savings from lower operating costs, the ability to provide greater freeze protection without adverse effects provide an opportunity to design a GSHP system with a lower EWT_{min}. Here, we compare the sizing of a vertical borehole heat exchanger when using the customary criterion of a minimum entering water temperature (EWT_{min}) of 32°F with a more aggressive criterion of an EWT_{min} of 25°F. To the extent that the customary minimum entering water temperature in the United States of 32°F is due, in part, to the common use of propylene glycol, consideration of other safe antifreezes warrants a reevaluation of this norm. The ANSI-CSA guideline recommends a design EWT_{min} of no less than 22°F below the mean ground temperature (see C448.2-16 section 7). When ground temperatures range from 54 to 45°F, as they do in NYS then, according to the ANSI-CSA design guidelines, the design EWT_{min} can range from 32 to 23°F.

The team includes methanol (MeOH) in our analysis as the fluid properties are similar to Kilfrost GEO and, by illustrating the similarities, it enables the use of MeOH as a proxy in commonly used sizing software. is beyond the scope of this project to consider all facets of a lower design EWT_{min}, our main interest is to illustrate the potential benefits of using an antifreeze that maintains a low viscosity under very cold ground loop conditions.

Figure 20. Flow Rate Ranges for Methanol, Propylene Glycol, and Kilfrost GEO in Straight Pipe in comparison to Figures 1 and 18

Note the fluid temperature coincides with a EWT_{min}, of 25°F (LWT of 20°F) and all antifreeze solutions have a freeze protection of 15°F.
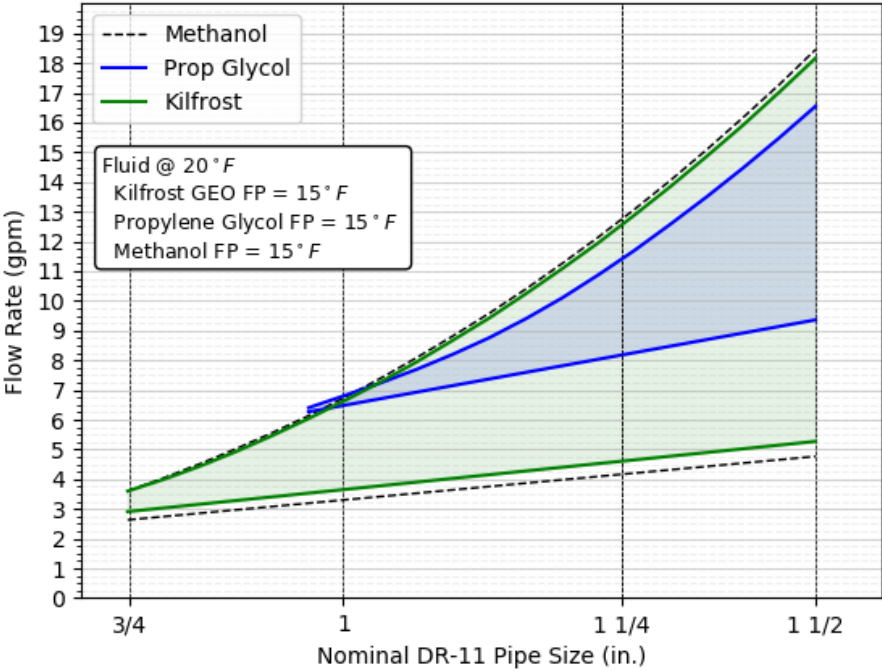
One potential benefit is the ability to design a ground loop to a colder EWT_{min} and reduce the size of the ground loop. As shown in Figure 20, the differences between antifreeze solutions increase for colder design temperatures that require more freeze protection. Under these conditions, the operating range for propylene glycol requires pipe sizes that are at least one-and-a-quarter inch and, even then, the range of flows is small.

For this analysis, we use the sizing software GLEHPro-v5 that allows for considerable control in specifying antifreeze solutions, including the addition of solutions not commonly used, such as Kilfrost GEO. To illustrate the impact of EWT_{min} on ground loop sizing, a sizing analysis was conducted using hourly load observations from a 4-ton (2 stage) heat pump in a single-family residence in the Northeast that were aggregated into monthly and peak loads (Table 11). The vertical sizing of the ground loop assumed a single u-bend of one-and-a-quarter inch DR11 pipe in a 6-inch borehole with the borehole thermal resistance of 0.304°F or Btu/(hr·ft), an "average rock" thermal conductivity of 2.0 Btu/(hr·ft·°F), and a deep earth temperature of 50°F.

Table 11. Heating and Cooling Loads for Ground Loop Sizing

Month	Total Heating [1000 BTUs]	Total Cooling [1000 BTUs]	Peak Heating [MBTU/hr]	Peak Cooling [MBTU/hr]
January	17,730	-	38.5	-
February	11,519	-	38.3	-
March	11,144	-	31.6	0.1
April	8,075	-	28.8	-
May	1,072	-	28.4	-
June	279	1,126	30.4	31.4
July	-	3,417	-	30.2
August	-	3,555	-	28.1
September	449	1,031	13.6	23.8
October	2,473	200	28.3	31.4
November	8,651	-	37.4	-
December	15,241	-	38.5	-

The temperature-dependent fluid properties for propylene glycol and methanol are included in GLHEPro and the properties for Kilfrost GEO were added at the temperature of interest. The fluid properties used in the sizing calculations are shown in Table 12.

Table 12. Fluid Properties Used in GLHE Pro Simulations

Antifreeze	Freeze Point [°F]	Temperature at Peak [°F]	Fluid Density [lb/ft³]	Volumetric Heat Capacity [Btu/(°F·-ft³)]	Thermal Conductivity [Btu/(hr·ft-F)]	Viscosity [lbm/(ft·hr)]
Propylene Glycol	20.0	29.0	63.78	60.63	0.278	9.995
Methanol	15.0	22.0	61.60	60.67	0.283	9.078
Kilfrost GEO	15.0	22.0	68.98	56.85	0.250	10.136

The results of the GLHE Pro sizing calculations (Table 13) suggest that a reduction of the EWT_{min} used in system design could result in a 27% reduction in the length of a vertical borehole heat exchanger.

Table 13. Results of GLHE Pro Simulations

Antifreeze Freeze Point	Design Minimum EWT	Avg Temperature at Peak Conditions	Borehole Length [feet]	% Reduction Relative to PG-20°F
PG - 20°F	32°F	29°F	539	--
MeOH -15°F	25°F	22°F	394	27%
GEO - 15°F	25°F	22°F	394	27%

To augment the GLHEPro analysis, the WaterFurnace GeoLink software was used to evaluate heat pump coefficient of performance (COP) and operating costs, to account for the lower temperature tendency to reduce the COP of the heat pump. The impact on energy use (kWh) and operating cost tends to be minimal and within a reasonable range. A WaterFurnace GeoLink software simulation compared a 4-ton heat pump with a ground loop sized for two different EWTs of 32°F and 25°F. The annual heating COPs came out to 4.35 and 4.20 for the EWTs of 32°F and 25°F respectively, resulting in an operating cost difference of ~$2.40/month. The required vertical heat exchanger to meet the design conditions was 545 feet versus 395 feet for the 32°F and 25°F cases; a 28% decrease in vertical bore needed. At a fully loaded $25/foot of finished closed loop vertical bore, that is, a savings of $3,750 for the project.

This comparison of Kilfrost GEO characteristics with propylene glycol shows that the advantage of using the newer fluid that enables a lower minimum EWT could be a saving of around 30% in the need for borehole drilling.

4.3 System Reliability

A key factor in the increase adoption of GSHP technology is to continue to build confidence in the technology through demonstration of quality installations and minimizing the number of installations that encounter problems.

In a recent NYSERDA report,[3] one lender is quoted: "A few bad projects can spoil perspectives of these technologies; however, it is not possible to avoid a bad story when you get to scale—we must be prepared to accept that." While so-called "bad projects" are inevitable, measures should certainly be taken to avoid them and their negative effects. Bad projects can include many different types of undesired outcomes that can have many different causes. One class of bad projects stems from inadequate heat transfer with the ground loop, potentially causing the system to rely on electric resistance heating, resulting in significant cost to the homeowner and a much higher impact on the electric grid.

The potential causes of inadequate heat transfer with the ground loop are numerous and include, for example, lower-than-expected thermal properties of the ground loop heat exchanger and laminar flow of the heat-conveying fluid in the ground loop piping.

Here we investigate the effects of increased fluid viscosity on the performance of the ground loop in terms of the ground loop fluid temperature. First, we simulate the effect of cold fluid viscosity on the ground loop temperatures to illustrate the added reliability that is provided when the viscosity of the antifreeze solution has a small dependence on temperature (i.e., Kilfrost GEO) compared to an antifreeze solution that has a larger change in viscosity at colder temperatures (i.e., propylene glycol). Then, we use the same simulation approach to explore (1) how uncertainty in thermal conductivity might affect ground loop performance for the two antifreeze solutions and (2) a range of ground loop flow rates, where below-design flow rates may result from incorrect pump speed settings, mechanical failure of a pump head, or splitting of flow between multiple ground loop circuits. If the lower flow rates and increased viscosity result in laminar flow conditions, the heat exchange with the ground will diminish, causing the fluid temperature to decrease further and potentially resulting in the system dropping below its freeze point.

4.4 Convective Heat Transfer

In designing GSHP systems, it is usually recommended to design pipe sizes and flow rates so that the flow in the ground loop heat exchanger remains turbulent for enhanced heat transfer with the ground. This is illustrated in Figures 1 and 18. Gehlin and Spitler (2015) and Gagne-Boisvert (2017) both investigated the effects of laminar flow on ground loop performance and found modest differences in system performance or operating cost. However, they considered ground loop temperatures above 30°F where differences in fluid viscosity are small. Here we consider the effect of colder loop temperatures that may arise due to these representative common design conditions, which do not consider the less common condition when a system operates below its designed minimum temperature (e.g., 32°F).

In addition to traditional sizing of pipes and determination of design flow rates, we consider conditions when the flow may be below the design value. For example, many installations rely on two pump heads to circulate fluid through the ground loop at flow rates that will maintain turbulent flow conditions. If a pump head fails, or one or more pump heads are set to the wrong speed, the time the fluid spends in the heat pumps evaporator is extended, potentially cooling the fluid below the freeze protection levels. The flow may also become laminar, resulting in poorer heat exchange, and cause the heat pump to go into a fault condition due to low pressure in evaporator. In all cases, as the fluid temperature decreases, the antifreeze solution will become more viscous and may lead to system failure.

As observed in the experiments, the difference in viscosity plays a relatively minor role in energy savings because the pressure drop in pipes under turbulent flow conditions depends on the fourth root of the viscosity. The main advantage of maintaining turbulent flow is to enhance heat transfer between the ground and fluid in the loop. When flow in a pipe is laminar, a well-defined boundary layer is established between the bulk fluid in the pipe and the wall of the pipe, impeding heat transfer. This convective resistance (Rc) adds to the borehole thermal resistance and is (from Lamarche et al., 2010):

$$R_c = \frac{1}{4\,\pi r h}$$

where h is the convective transfer coefficient, given by Incropera et al (2002) as:

$$h = Nu \cdot k_{fluid}/d_{pipe}$$

with k_{fluid} as the thermal conductivity of the fluid and d_{pipe} as the inside diameter of the pipe. For turbulent flow in straight pipes with Reynolds numbers greater than 3000, the Nusselt number (Nu) is obtained from the Gnielinski correlation (Incropera et al, 2002):

$$Nu = \frac{(f/8) \cdot (Re - 1000) \cdot Pr}{1 + 12.7\sqrt{f/8} \cdot (Pr^{2/3} - 1)}$$

For laminar flow in straight pipes with Reynolds numbers less than 2300, the Nusselt number is constant and 4.36 is used (following Gehlin & Spitler, 2015). For the transition region between laminar and turbulent flow, a linear interpolation is used. Based on the fluid properties of Kilfrost GEO at 30% concentration, the Prandtl number (Pr) is taken as a constant value of 25.

To explore the dynamic effects of the convective resistance on ground loop performance and system reliability, we use a modeling approach, similar to Gehlin and Spitler (2015 and Gagne-Boisvert (2017). Here, the model uses measured heat of extraction in residential heat pump system with a 4-ton two-stage water-to-air heat pump. The measured heat of extraction is then fixed and used to calculate the thermal response of the ground at the borehole wall using the line source model (Carslaw and Jaeger,1959). This characteristic response function (B) is then combined with the measured heat of extraction as the forcing function (F) using Duhamel's theorem (e.g., Olsthoorn, 2008, Marcotte and Pasquir, 2008, Lamarche, 2009; Zhang et al., 2011) to compute the ground temperature (T_g) as a function of time (t).

$$T_g(t) = \int_{\tau=0}^{\infty} F(t - \tau) g(\tau) d\tau$$

The calculations are performed numerically using the Python SciPy package (Virtanen et al., 2020).

The temperature of the fluid in the ground loop heat exchanger (T_f) is then computed by subtracting from the ground temperature at the borehole (Tg) the thermal losses due to the borehole thermal resistance (R_b) and the rate of heat extraction (q_{HE}):

$$T_f(t) = T_g(t) - R_b \cdot q_{HE}$$

Borehole resistance has three components, the thermal resistance of the pipe (R_p) and the grout (R_{grout}) and the thermal convective resistance R_c. The pipe and grout resistances are summed and held constant. For DR-11 HDPE pipe in a grout with a thermal conductivity of 0.81 Btu/(hr·ft·°F), the sum of the pipe and grout resistance terms (R_p and R_{grout}, respectively) is 0.208 °F/[Btu/(hr·ft)], using the equations in section 5.2.2.3 of the IGSHPA (2011). These values are similar to those used by Gagne-Boisvert and Bernier (2017).

Each simulation begins with a computation of the ground temperature (T_g) (Figure 21) using a representative time series of heat of extraction/rejection. Using the ground temperature as an approximation of the fluid temperature, the fluid viscosity and Reynolds Numbers are calculated. These values are then used to calculate the convective resistance (R_c) term. The total borehole resistance is then used to calculate the temperature of the fluid in the ground loop (T_f). This process is repeated for each value of ground temperature to result in a time series of fluid temperatures. The model is relatively simple in that it does not account for changes in heat of extraction that result from decreases in fluid temperature. Likewise, the calculations do not consider the effects of the fluid freezing when the simulated temperature drops below the freeze protection limit. The main objective is to explore the effects of fluid temperature, viscosity, and convective resistance on the dynamic behavior of a GSHP system.

**Figure 21. Ground Loop Simulation Flow Chart**
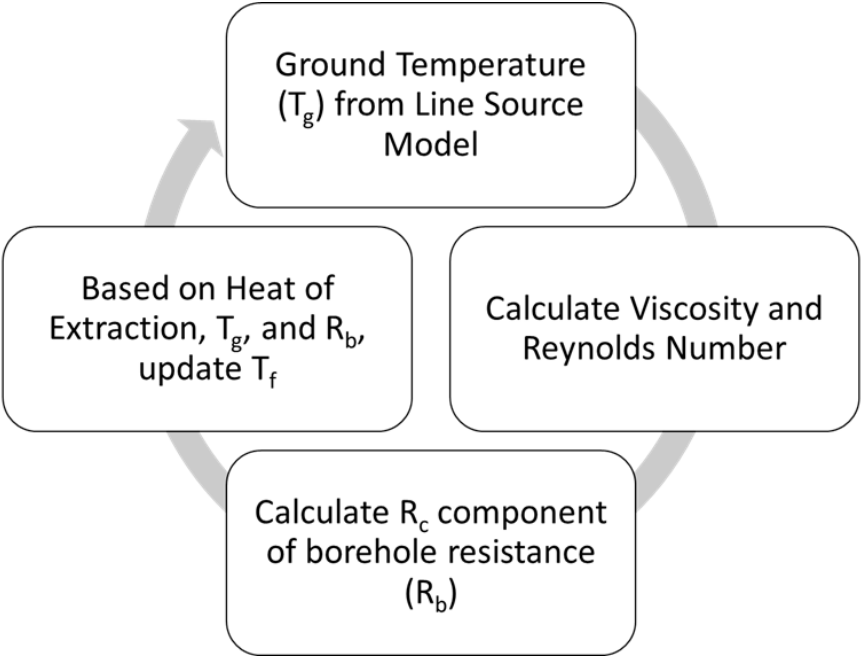
Because the interest is in the response during events when the ground loop is expected to get very cold, we focus on measurements from October 1, 2017, through January 31, 2018, and specifically for a 15-hour period on December 27, 2017, when the outdoor temperature fell below the design temperature (-2 °F) and remained below that temperature for more than 24 hours.

The first simulation (Figure 22) represents the base case with a pumping rate of 12 gpm and show that there is little difference between the two antifreeze solutions (both with freeze protection to 15°F). Even though the propylene glycol has a higher viscosity and correspondingly lower Reynolds number, flow remains turbulent and there is no effect on the convective resistance (R_c). In this base case scenario, the leaving water temperature drops to approximately 22°F, which coincides with a design minimum EWT of 25°F.

Figure 22. Simulated Ground Loop Conditions, Example 1

For system described in text with a constant flow rate of 12 gpm for conditions when outdoor air temperature dropped below design temperature of -2 °F.
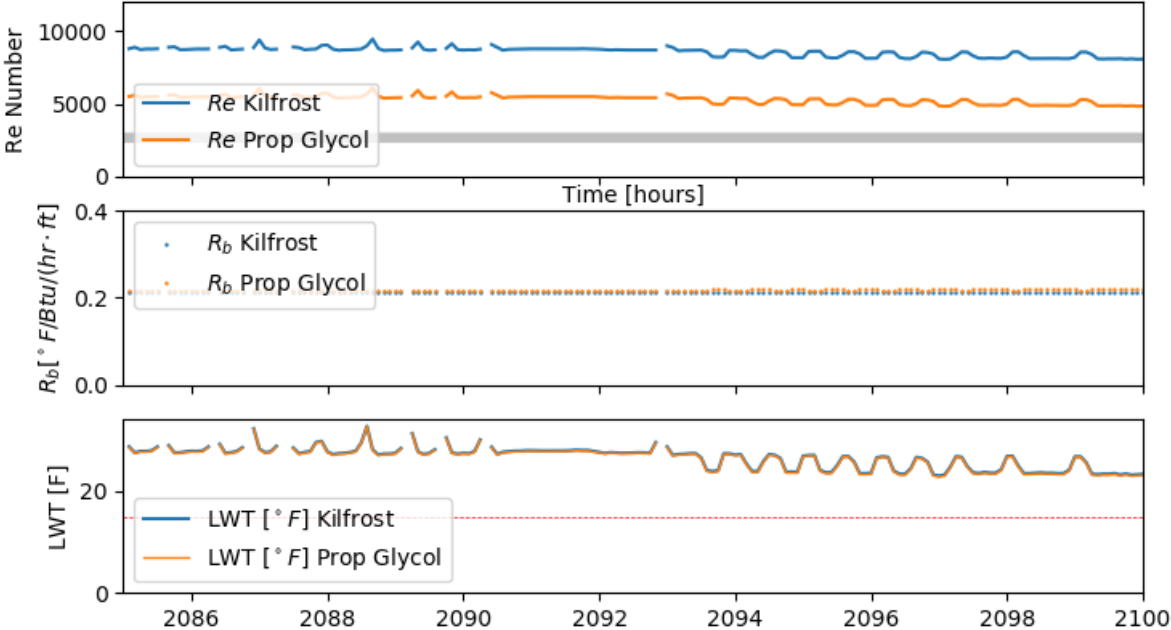

The second simulation uses the same input data with the only exception being that the flow rate is reduced by 50%, to 6 gpm. This may coincide with an improper setting of the pump speeds or a mechanical failure of the one of the pump heads, either case would likely go unnoticed under typical operating conditions and would only become apparent when the loop temperature reached its design limit. The results of the second simulation (Figure 23) shows that at lower flow rates, the increased viscosity of propylene glycol results in the flow transitioning to laminar and thus increasing the convective resistance. This then causes an increase in the borehole resistance (R_b) resulting in a greater thermal drawdown in the borehole. The lower flow rate also increases the temperature drop across the heat pump and the ground loop temperature drops below the freeze protection limit.

These results are consistent with the findings of Gagne-Boisvert and Bernier (2017) and Gehlin and Spitler (2015). However, in those studies, they did not consider ground loop temperatures below 30 °F.

Figure 23. Simulated Ground Loop Conditions, Example 2

For system described in text with a constant flow rate of 6 gpm for conditions when outdoor air temperature dropped below design temperature of -2 °F.
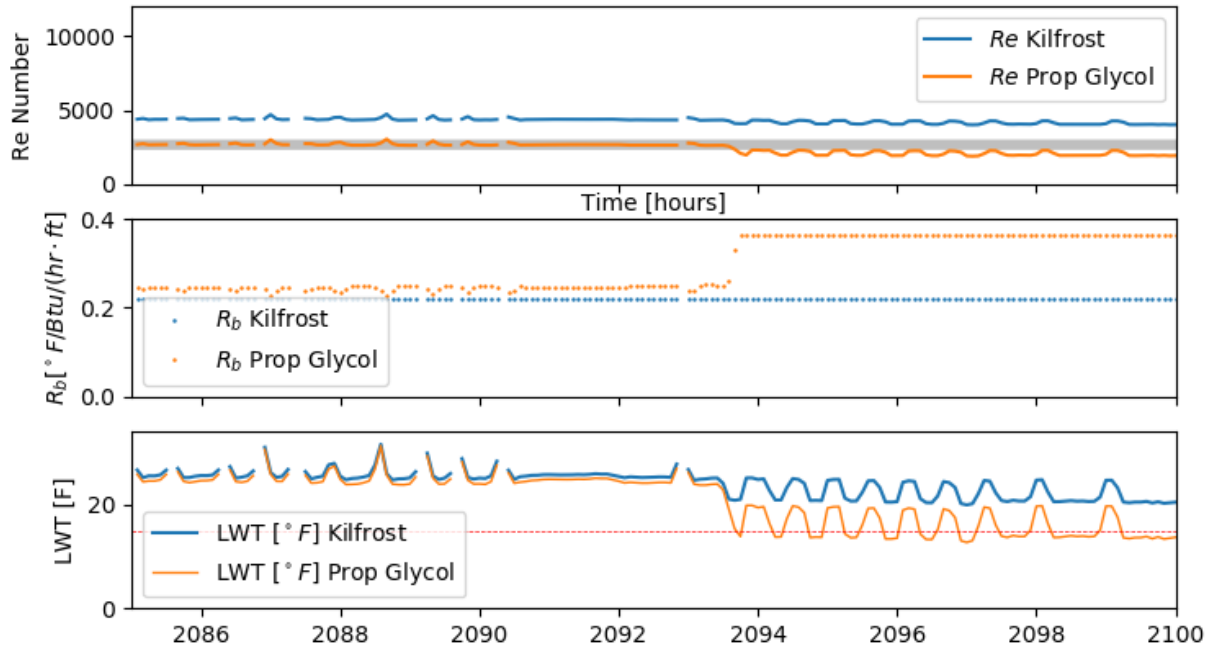

4.4.1 Uncertainty in System Design and Operation

To evaluate the sensitivity of the ground loop performance on ground loop flow rate and the ground thermal conductivity, a sensitivity analysis is conducted that applies multipliers on flow rate and thermal conductivity to consider a range of hypothetical conditions. Uncertainty in thermal conductivity is represented as a range of values from 1 to 1.8 Btu/(hr·ft·°F). According to the IGSPHA design documents (EPRI, 1989), crystalline igneous rocks range from approximately 1 to 2.5 Btu/(hr·ft·°F), so 1.8 is taken as an intermediate value that might be used in a design and 1.0 as the lower limit of the expected range. Likewise, below-design ground loop flow rates range from 50% to 100% of the design flow, or in this case 6 to 12 gpm. Below-design flow rates may be due to the failure of a pump head (e.g., in a two-pump system), improper speed settings on the fixed-speed pump speed, or problems with controls on a variable speed pump.

Figure 24. Contour Plots of Minimum Leaving Water Temperatures

For a range of flow rate and thermal conductivities for propylene glycol (upper) and Kilfrost GEO (lower). Shaded areas denote conditions for which LWT drops below freeze protection.
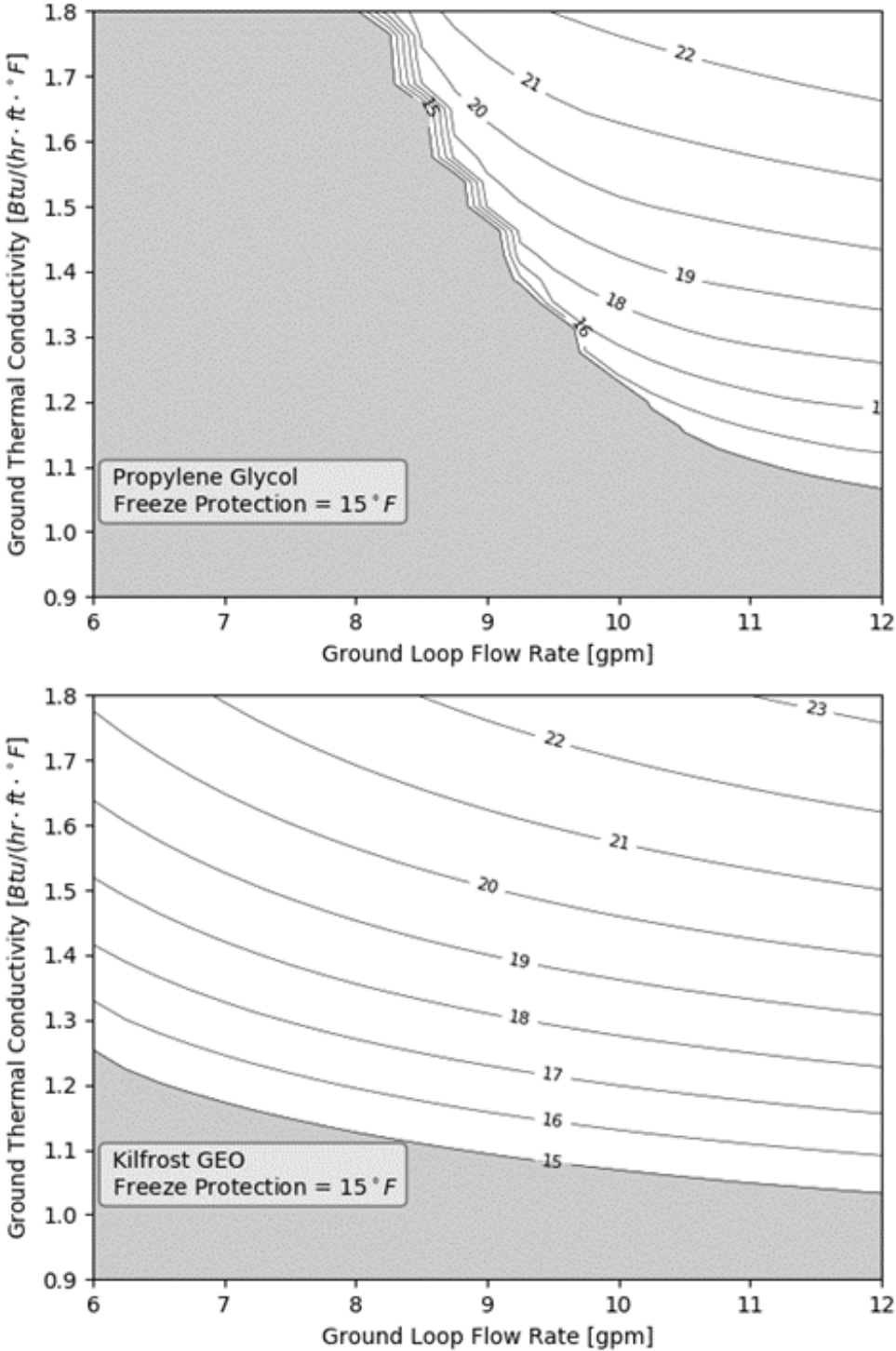
The purpose of this analysis is to assess how much variation in these parameters can be tolerated under a stressed condition without the ground loop dropping below the freeze protection limit. For each pair of ground loop flow rate and ground thermal conductivity values, the line source model is applied to the example time-varying heat of extraction that was used in the previous analyses for the period October 1, 2017 to January 31, 2017. This period includes the very cold weather event in the last week of December 2017 when the outdoor temperature dropped below the design temperature.

As shown in Figure 24, the LWT for both propylene glycol and Kilfrost GEO are similar, though when the flow rates multiplier drops below 8 gpm, the propylene glycol temperatures are impacted by low Reynolds numbers and higher borehole resistances, resulting in lower temperatures. The shaded areas denote conditions where the calculated leaving water temperature drops below the freeze protection level. The greater level of freeze protection provided by Kilfrost GEO provides a greater level of reliability to the operation of a GSHP system. While greater freeze protection can be provided by propylene glycol, the adverse viscosity effects become more pronounced.

5   Conclusions

The project team has successfully designed, constructed, and operated experimental equipment to mimic a GSHP system, and used this to quantify differences between a standard propylene glycol-based fluid and Kilfrost GEO.

The experimental results showed differences in performance between propylene glycol and Kilfrost GEO which were demonstrated to be due to the lower viscosity of Kilfrost GEO solutions, resulting in the need for lower pumping power.

An empirical multidimensional model was developed by Kilfrost that was confirmed in the experimental trials and used in a set of numerical analyses to compare antifreeze solutions under a wider range of conditions.

Although a strong temperature dependence of viscosity has adverse effects for system operation, Kilfrost GEO maintains a wider operating window of flow rates over a range of freeze protections and fluid temperatures when compared to propylene glycol solutions.

For typical operating conditions in the Northeast United States, Kilfrost GEO can provide a freeze protection of 15°F while using 6% less electricity for ground loop pumping than propylene glycol with a freeze protection of 20°F.

When comparing Kilfrost GEO with propylene glycol at the same 20°F freeze point, electricity savings would range from 11 to 15%.

The ability to provide for freeze protection to 15°F and operate at colder temperatures without the adverse effects of propylene glycol provides a potential opportunity to reduce drilling depths and related costs by as much as 27%. These results are based only on computer simulations and should be validated with actual field testing prior to being adopted as a new design practice.

Kilfrost GEO is likely to maintain fluid turbulence (and hence more favorable heat transfer) and better freeze protection (through turbulent flow) than propylene glycol, leading to greater system reliability and providing less risk to system owners, designers, installers, and investors.

6   References

ANSI/CSA (2016), Design and installation of ground source heat pump systems for commercial and residential buildings, American National Standards Institute, Canadian Standards Association, ANSI/CSA C448 Series-16, 211pp.

Carslaw, H.S. & Jaeger, J.C. (1959). Conduction of heat in solids, 2nd Ed., Oxford Press, 510 pp.

Casasso, A. & Sethi, R. (2014). Efficiency of closed loop geothermal heat pumps: A sensitivity analysis. *Renewable Energy, 62,* 737-746.

CDH Energy (2018). Analysis of Water Furnace geothermal heat pump sites in New York State with Symphony monitoring system: Final Report, NYSERDA, 106 pp.

Cheng, P., Gui, N., Yang, X., Tu, J., Jiang, S., & Jia, H. (2020). A numerical investigation on single-phase flow characteristics and frictional pressure drop in helical pipes. In *Fluid Dynamics Research* (Vol. 52, Issue 4, p. 045505). https://doi.org/10.1088/1873-7005/ab993f

Clauser C. & Huenges, E. (1995). Thermal conductivity of rocks and minerals, in Rock Physics and Phase Relations, A Handbook of Physical Constants, American Geophysical Union, p 105 – 126.

Dursky and ERS (2019). Renewable Heating and Cooling Financial Solutions Market Research, Final Report.

Gagné-Boisvert, L., & Bernier, M. (2017, March). A comparison of the energy use for different heat transfer fluids in geothermal systems. *IGSHPA Technical/Research Conference and Expo*.

EPRI, 1989, Soil and rock classification for the design of ground-coupled heat pump systems: Field Manual, Electric Power Research Institute, Palo Alta, California, 55 pp.

Gehlin, S. E. A., & Spitler, J. D. (2015). Effects of Ground Heat Exchanger Design Flow Velocities on System Performance of Ground Source Heat Pump Systems in Cold Climates. *ASHRAE Winter Conference*, 24–28.

Ju, H., Huang, Z., Xu, Y., Duan, B., & Yu, Y. (2001). Hydraulic Performance of Small Bending Radius Helical Coil-Pipe. *Journal of Nuclear Science and Technology*, *38*(10), 826–831.

IGSHPA (2011), Ground Source Heat Pump Residential and Light Commercial Design and Installation Guide, Oklahoma State University, 560 pp.

Incropera, F.P., Dewitt, D.P., Bergman, T.L., and Lavine, A.S. (2002). Fundamentals of Heat and Mass Transfer, 5th Edition, John Wiley & Sons, Inc., New York.

Lamarche, L. (2009). A fast algorithm for the hourly simulations of ground-source heat pumps using arbitrary response factors. *Renewable Energy*, *34*(10), 2252–2258.

Lamarche, L., Kajl, S., & Beauchamp, B. (2010). A review of methods to evaluate borehole thermal resistances in geothermal heat-pump systems. *Geothermics*, *39*(2), 187–200.

Marcotte, D., & Pasquier, P. (2008). Fast fluid and ground temperature computation for geothermal ground-loop heat exchanger systems. *Geothermics*, *37*(6), 651–665.

Olsthoorn, T.N. (2008), Do a bit more with convolution, Ground Water, 46(1), 13-22.

Seabold, Skipper, and Josef Perktold. (2010) statsmodels: Econometric and statistical modeling with python. *Proceedings of the 9th Python in Science Conference.* 2010.

Spitler and others, (2016), GLHEPro 5.0 for Windows User's Guide, International Ground Source Heat Pump Association, 156pp.

Virtanen, P., and others (2020), SciPy 1.0: Fundamental algorithms for scientific computing in Python, Nature Methods, 17(3), 261-272.

Zhang, Y., Pan, L., Pruess, K., & Finsterle, S. (2011). A time-convolution approach for modeling heat exchange between a wellbore and surrounding formation. *Geothermics*, *40*, 261–266.

Appendix A. Temperature Sensor Calibration

Temperature sensors were calibrated over an extended range (-6 °Cto 6 °C) by clustering the six DS18B20 One-Wire sensors around the reference thermometer (QTI DTU6005 USB thermometer) and submerging the cluster into an aqueous bath subjected to a range of temperatures. The temperature sensors are clustered together with wire ties and wrapped in thermal insulation so that the primary contact of all sensors is co-located at the bottom of the bath. The cluster was affixed to a stationary blade and inserted into the test solution. The constant temperature bath consists of a Cuisinart ice cream maker with a rotating fluid-filled drum and a stationary stirring blade. The fluid in the annulus of the drum provides good thermal stability and a degree of thermal insulation from the surrounding environment. The rotation of the drum at approximately (40 rpm) around the stationary blade helps to keep the solution well mixed and avoids stratification.

The reference thermometer (shown in center) is a QTI USB Thermometer with a rated accuracy of 0.1°C. The test solution was brought to -6°C by placing it in a freezer for several hours. Normally, the tank will warm to room temperature over a period of several hours allowing for a gradual increase in temperature over the range of interest. However, because the tank annulus and the working fluid were both chilled, the change in tank temperature was very slow (approximately 1°C over a 1-hour period). The tank temperature was adjusted incrementally by injecting 20cc of hot water slowly into the top of the tank, raising the tank temperature approximately 1°C over a 5-minute period. For each transition, the initial 2 minutes of data was removed as transient effects were prominent.

The regression equations are used to correct each temperature measurement to the common 'reference' value prior to calculating a ΔT. For example, if sensor G11552 measures a temperature of -2.00 °C, the value is corrected by subtracting the correction of 0.045 (δT = (-0.011)*(-2.00) + 0.023) to arrive at a corrected measurement of -2.045 °C.

Upon correction, each temperature sensor has a residual error relative to the reference thermometer that is characterized by the root-mean-square-error (RMSE) of the regression (noted on figures). The RMSE for the six sensors is approximately 0.02 °C. Measurement error of ΔT that results from error in temperature sensors can be estimated as the root sum of square errors:

$$\delta \varDelta T \;=\; \sqrt{(\delta T_1)^2 + \ (\delta T_2)^2} \simeq 0.028°\text{C}$$

Appendix B. Repeated Run for Propylene Glycol

An additional experimental run was conducted to evaluate the repeatability of the experimental apparatus and procedures. Propylene glycol was selected for the replicate.

The results indicate that the repeated trials of propylene glycol resulted in statistically significant correlations between parameters. The regression slopes for the correlations (Tables 4, 6, and 8 compared with Tables B1, B2, and B3) are not statistically different, indicating that the observed trends are repeatable.

While the correlation slopes are essentially the same, the repeated run of propylene glycol exhibited a slightly higher pressure drop and pumping power than the original run over the same range of temperatures. At a temperature of 25 °F, the difference in pumping power between Tasks 5 and 10 is 5.3% and the difference in pressure drop is 2.0%. Similarly, for a pressure drop of 18.5 psi, the pumping power in Task 10 is 3.2% higher than that of Task 5. The differences between Tasks 5 and 10 (2-5%) are within a reasonable range of repeatability and are much less than the differences between propylene glycol and Kilfrost GEO.

Table B-1. Summary Statistics for Pumping Power versus Loop Temperature, Task 10

| Pump Power versus Loop Temperature: Task 10 (Antifreeze #1)					
No. Observations	36		R-squared		0.988
Df Residuals	34		F-statistic		2846.
Df Model	1		Prob (F-statistic)		2.30e-34
coeff		Std err	t	P>|t|	$CI_{0.025}$	$CI_{0.975}$
Intercept	500.833	2.282	219.435	0.000	496.195	505.471
Slope	-4.664	0.087	-53.346	0.000	-4.841	-4.486

Table B-2. Summary Statistics for Pumping Power versus Pressure Drop, Task 10

Pump Power versus Pressure Drop: Task10 (Antifreeze #1)					
No. Observations	36		R-squared		0.993
Df Residuals	34		F-statistic		4833..
Df Model	1		Prob (F-statistic)		3.06e-38
coeff		Std err	t	P>|t|	$CI_{0.025}$	$CI_{0.975}$
Intercept	-43.3558	6.125	-7.079	0.000	-55.802	-30.909
Slope	22.5977	0.325	69.522	0.000	21.937	23.258

Table B-3. Summary Statistics for Pressure Drop versus Loop Temperature, Task 10

Pressure Drop versus Loop Temperature: Task 10 (Antifreeze #1)					
No. Observations	40		R-squared		0.989
Df Residuals	38		F-statistic		3279.
Df Model	1		Prob (F-statistic)		1.71e-38
coeff		Std err	t	P>|t|	$CI_{0.025}$	$CI_{0.975}$
Intercept	24.076	0.094	256.056	0.000	23.886	24.267
Slope	-0.206	0.004	-57.265	0.000	-0.213	-0.199

Figure B-1. Time Series Plots for Repeated Propylene Glycol Run
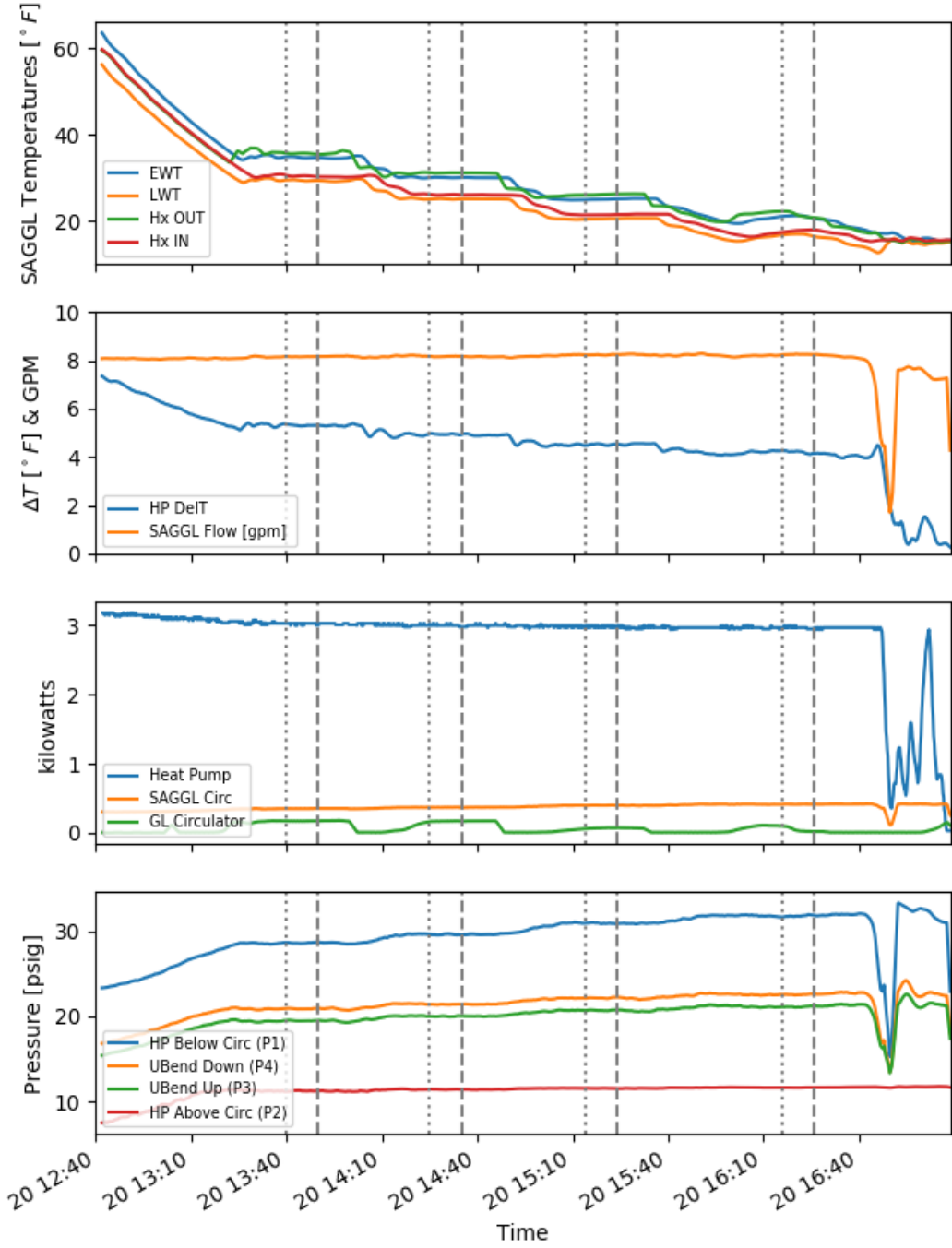
Appendix C. Friction Factors

As noted, as the experimental conditions in this study span different hydraulic conditions, the comparison becomes slightly more difficult ("apples and oranges"). However, by applying the Darcy Weisbach theory and using models of friction coefficient appropriate for the flow conditions, we are able to provide a theoretical explanation for the experimental observations.

C.1   Straight Pipe

For laminar flow, f is simply $64/Re$, where Re is the Reynolds number. As a result, in the laminar flow regime the frictional factor and thus the pressure drop are linearly related to the Reynolds number. Because the Reynolds number is inversely related to viscosity, the pressure drop is then directly (and linearly) related to viscosity -- higher viscosities resulting in higher pressure drop.

However, in the turbulent flow regime, pressure drop is less dependent on viscosity. There are many representations of the friction factor (f) for turbulent flow and these are often plotted on Moody diagrams. One commonly used form is the Colebrook equation[4]:

$$\frac{1}{\sqrt{f}} = -2.0 \, log(\frac{(\epsilon/d)}{3.7} + \frac{2.51}{Re\sqrt{f}})$$

where ϵ is the roughness coefficient and d is the pipe diameter. Note that because f appears on both sides of the equation, an iterative solution is required. Another representation of the friction factor in straight pipes that spans both the laminar and turbulent flow regimes is the Churchill equation:

$$f = 8[\,(\frac{8}{Re})^{12} + \frac{1}{(A+B)^{1.5}}]^{\frac{1}{12}}$$

$$A = [2.457 \cdot ln(\frac{1}{(\frac{7}{Re})^{0.9} + 0.27\,\frac{\epsilon}{D}})]^{16}$$

$$B = (\frac{37530}{Re})^{16}$$

The Churchill equation is applied in our analysis of the vertical borehole heat exchangers below.

C.2 Coiled pipes

For laminar flow in coiled pipes, we use the equation of Srinivasan et al (1970) that applies a correction factor to the straight-pipe friction coefficient of $f_s=64/Re$. The Srinivasan equation is valid for Dean numbers greater than 300 and λ between 0.01 and 0.14 (Ghobadi and Muzychka, 2016). Recall that λ for SAGGL is 0.027.

$$f_c = (64/Re) \cdot 0.1125 De^{0.5}$$

For turbulent flow, we use the equation of Ju et al (2001) that is valid for Reynolds numbers greater than Re_{crit} (4700) and Dean numbers greater than 11.6. Both conditions are met for Kilfrost GEO.

$$f_c = (0.316/Re^{0.25}) \cdot (1 + 0.11 Re^{0.23}) \cdot \lambda^{0.14}$$

Table C-1. Summary of Friction Factors for Different Pipe Geometries and Flow Conditions

Pipe Geometry	Flow condition	Equation	Source
Coiled	Laminar	$f_c = (64/Re) \cdot 0.1125 De^{0.5}$	Srinivasan (1970)[a]
Coiled	Turbulent	$f_c = (0.316/Re^{0.25}) \cdot (1 + 0.11 Re^{0.23}) \cdot \lambda^{0.14}$	Ju et al (2001)
Straight	Laminar	$f = 64/Re$	Fay (1994)
Straight	Turbulent	$\frac{1}{\sqrt{f}} = -2.0 \, log(\frac{(\epsilon/d)}{3.7} + \frac{2.51}{Re\sqrt{f}})$	Fay (1994)
Straight	Laminar Transition Turbulent	$f_s = 8[(\frac{8}{Re})^{12} + \frac{1}{(A+B)^{1.5}}]^{1/12}$ $A = [2.457 \cdot ln(\frac{1}{(\frac{7}{Re})^{0.9} + 0.27\frac{\epsilon}{D}})]^{16}$ $B = (\frac{37530}{Re})^{16}$	Churchill (1977)[b]

[a]   As cited by Ghobadi and Muzychka (2016).

[b]   Churchill, SW, 1977, Friction factor equation spans all fluid-flow ranges. Chem Eng 84, 91-92.

Endnotes

[1] SciPy documentation https://docs.scipy.org/doc/scipy/reference/generated/scipy.stats.kruskal.html

[2] Note that another form of the Darcy-Weisbach equation differs by a factor of four. For example, see Holland, F. A., and R. Bragg. *Fluid Flow for Chemical Engineers*, Elsevier Science & Technology, 1995. Here, we use the form that coincides with straight pipe laminar flow friction factor of 64/Re, instead of 16/Re and subsequent equations are consistent with this form.

[3] Renewable Heating and Cooling Financial Solutions Market Research, 2019, Final Report, Dunsky and ERS.

[4] Fay, J.A, 1994, Introduction to Fluid Mechanics, MIT Press, 605 pp.

NYSERDA, a public benefit corporation, offers objective information and analysis, innovative programs, technical expertise, and support to help New Yorkers increase energy efficiency, save money, use renewable energy, and reduce reliance on fossil fuels. NYSERDA professionals work to protect the environment and create clean-energy jobs. NYSERDA has been developing partnerships to advance innovative energy solutions in New York State since 1975.

To learn more about NYSERDA's programs and funding opportunities, visit nyserda.ny.gov or follow us on Twitter, Facebook, YouTube, or Instagram.